ORIGINAL RESEARCH

Expression of Normally Repressed Myosin Heavy Chain 7b in the Mammalian Heart Induces Dilated Cardiomyopathy

Angela K. Peter, PhD;* Alberto C. Rossi, PhD;* Massimo Buvoli, MD, PhD; Christopher D. Ozeroff, BA; Claudia Crocini, PhD; Amy R. Perry, BS; Ada E. Buvoli, BS; Lindsey A. Lee, BS; Leslie A. Leinwand, PhD

***Background*—**In mammals, muscle contraction is controlled by a family of 10 sarcomeric myosin motors. The expression of one of its members, MYH7b, is regulated by alternative splicing, and while the protein is restricted to specialized muscles such as extraocular muscles or muscle spindles, RNA that cannot encode protein is expressed in most skeletal muscles and in the heart. Remarkably, birds and snakes express MYH7b protein in both heart and skeletal muscles. This observation suggests that in the mammalian heart, the motor activity of MYH7b may only be needed during development since its expression is prevented in adult tissue, possibly because it could promote disease by unbalancing myocardial contractility.

***Methods and Results*—**We have analyzed MYH7b null mice to determine the potential role of MYH7b during cardiac development and also generated transgenic mice with cardiac myocyte expression of MYH7b protein to measure its impact on cardiomyocyte function and contractility. We found that MYH7b null mice are born at expected Mendelian ratios and do not have a baseline cardiac phenotype as adults. In contrast, transgenic cardiac MYH7b protein expression induced early cardiac dilation in males with significantly increased left ventricular mass in both sexes. Cardiac dilation is progressive, leading to early cardiac dysfunction in males, but later dysfunction in females.

***Conclusions*—**The data presented show that the expression of MYH7b protein in the mammalian heart has been inhibited during the evolution of mammals most likely to prevent the development of a severe cardiomyopathy that is sexually dimorphic. **(*J Am Heart Assoc*. 2019;8:e013318. DOI: 10.1161/JAHA.119.013318.)**

Key Words: cardiac dysfunction • cardiac myocyte • MYH7b • myosin heavy chain • transgenic mice

The 2 myosin motors expressed in mammalian cardiomyocytes are [α] and [β]-myosin heavy chains (MyHC)p. The relative ratio of these 2 isoforms determines the enzymatic activity of the thick filament which controls contractile velocity and force generation in both physiological as well as pathological conditions.[1–4] A potential link between transcription of a third sarcomeric myosin gene, MYH7b, and cardiac dysfunction remains ambiguous because of the lack of protein in the mammalian heart. MYH7b is an ancestral myosin gene which is most homologous to α- and β-MyHCs and encodes the intronic microRNA, mir499.[5,6] While the role of mir499 in controlling cardiac gene expression and mitochondrial fission has been well-documented,[7,8] the role of MYH7b in mammalian cardiac function remains elusive. In fact, MYH7b expression is regulated post-transcriptionally through tissue-specific skipping of exon 7 which encodes the myosin P-loop required for ATP binding and hydrolysis.[9] Exon 7 exclusion results in (1) disruption of the MYH7b open reading frame; (2) potential synthesis of a truncated protein product, and (3) partial degradation of the mRNA by nonsense-mediated decay (NMD).[9] Importantly, nuclear processing of microRNA precursors protects mir499 from NMD activity and uncouples host gene-microRNA co-expression. Furthermore, bioinformatic analysis of RNA elements and motifs involved in alternative splicing regulation suggests that exon 7 skipping is a conserved event occurring across many mammalian species.[9] More recently, a second alternative splicing pattern, which also affects MY7b protein expression, has been identified in chicken hearts. In this case, binding of the RNA binding protein CELF1 to the first intron of MYH7b pre-mRNA, promotes inclusion of an out-of-frame exon that causes an early arrest of protein translation.[10]

Consistently, MYH7b protein has either not been not been detected in mammalian hearts or at levels so low, that its

From the Department of Molecular, Cellular and Developmental Biology, Biofrontiers Institute, University of Colorado, Boulder, CO.

Accompanying Table S1 and Figures S1 through S8 are available at https://www.ahajournals.org/doi/suppl/10.1161/JAHA.119.013318

*Dr Peter and Dr Rossi contributed equally to this work.

Correspondence to: Leslie A. Leinwand, PhD, BioFrontiers Institute, University of Colorado Boulder, 3415 Colorado Ave., Boulder, CO 80303. E-mail: leslie.leinwand@colorado.edu

Received May 21, 2019; accepted June 26, 2019.

Clinical Perspective

What Is New?

- The specialized member of the sarcomeric myosin gene family, MYH7b, is not essential for mammalian cardiac development.
- Forced protein expression of MYH7b protein in the mammalian heart results in progressive dilated cardiomyopathy associated with decreased cardiac function.
- Our results support the idea that the MYH7b protein production has been evolutionarily silenced for protein production except in a small number of tissues.

What Are the Clinical Implications?

- Several genome-wide association studies have implicated the MYH7b gene in a variety of cardiovascular diseases.
- Although MYH7b protein is found in heart and skeletal muscles of birds and reptiles, expression of full-length active MYH7b protein had not been detected in mammalian hearts.
- Therefore, MYH7b mutations potentially linked to cardiac diseases can only produce their pathogenic effects through the gene's RNA.

significance is unclear.[6,11,12] In contrast, MYH7b protein is expressed in snake and chicken hearts and skeletal muscle (L.A. Leinwand, PhD, unpublished data, 2019).[6]

Splicing regulation provides an explanation for the initial puzzling finding of the widespread presence of the MYH7b transcript in different mammalian tissues despite undetectable levels of protein in most muscles.[9] In both rat and mouse, the protein is only found several fibers in the orbital layer of extraocular muscles, and in soleus muscle spindles but not in the heart.[6] Accordingly, exon 7 skipping analysis shows incorporation of exon 7 in the mature mRNA to be 40% in the soleus but only 4% in the ventricle.[9] Moreover, a more recent report of MYH7b protein being expressed in mammalian heart was subsequently corrected.[13] Thus, the expression of MYH7b protein has changed during evolution since it is easily found in heart and skeletal muscles of birds and reptiles (L.A. Leinwand, PhD, unpublished data, 2019).[6]

A survey of different human tissues confirmed the low level of exon 7 incorporation in striated muscle and heart, but revealed an unexpectedly high percentage of transcripts capable of encoding the functional full length protein in the brain (≈60%).[9] Consistent with this observation, screening for proteins that regulate synaptic function showed that MYH7b controls synaptic strength by modulating actin cytoskeleton arrangement within dendritic spines of cultured hippocampal neurons.[14] MYH7b pleiotropy has been also confirmed by a genetic study linking compound heterozygous mutations in different functional domains of MYH7b to hereditary sensorineural hearing loss (SNHL).[15] Interestingly, congenital myopathy coupled with left ventricular non-compact cardiomyopathy (LVNC) has also been associated with digenic inheritance of mutant ITGA7 and MYH7b genes.[16] LVNC is a rare cardiomyopathy which carries a substantial risk of heart failure, arrhythmia, and sudden death. The disease is characterized by spongy LV myocardium, persistence of ventricular trabeculations and the presence of extensive intratrabecular recesses.[17–22] However, it should be noted that in this study non-productive exon 7 skipping, which prevents expression of the full-length protein in both mouse and rat heart, was not examined. Additionally, expression of the MYH7b protein was not assessed; only the presence of the mRNA was probed. Although several authors have proposed that LVNC, at least in some patients, is a condition acquired postnatally,[23] there is strong evidence supporting the hypothesis that LVNC is caused by aberrant embryonic maturation of the LV that takes place during the transition from a non-vascularized and trabecular organization, to a mature compacted myocardium.[22] Thus, it seems reasonable to hypothesize that MYH7b protein could be produced only during cardiac embryogenesis and inactivated after birth. However, mass spectrometry-analysis performed on 17- to 23-week human fetal hearts, did not identify MYH7b in the ventricular proteome.[24]

Since the role of MYH7b in mammalian heart and skeletal muscle remains ambiguous, we assessed its potential but unexplored contribution to heart development by examining MYH7b null animals. The pups were born with expected genotypes. We also found no obvious defects in the hearts of adult MYH7b null animals at baseline. We tested the hypothesis that expression of MYH7b protein in the adult heart would be detrimental in a mouse model of forced transgenic expression of the MYH7b full-length cDNA. As hypothesized, mice expressing MYH7b protein in the heart exhibited early ventricular mass enlargement, dilation and contractile dysfunction in males and later dilation and contractile dysfunction in females.

Methods

The data that support the findings of this study are available from the corresponding author upon reasonable request.

Generation of MYH7b Global Null Mice

Mice were provided to the Leinwand Lab by Dr Eric Olson's laboratory at the University of Texas Southwestern and generated according to the protocol previously described.[25] In short, CRISPR/Cas9 was used to make a double stranded DNA break, and a triple Poly adenylation (PolyA) sequence was knocked in by homologous recombination into exon 2 of

the MYH7b gene. A guide RNA was designed to target the second exon of MYH7b (5′—TGATGGATATGAGTGAACTTGG—3′). A target vector ssODN with 3x PolyA flanked by a 5′ arm and 3′ arm around the gRNA site. Both Cas9 mRNA, sgRNA, and ssODN were injected into C57Bl/6 zygotes and transferred to pseudopregnant female mice. Tail biopsies were used for genotyping as described below to screen offspring for the presence of the PolyA sequence. All animal procedures were approved by the University of Colorado, Boulder, CO, Institutional Animal Care and Use Committee: animal protocol number 235116FEB2019.

Generation of MYH7b Transgenic Mice

The human *MYH7b* coding sequence from plasmid pF1KA1512 purchased from Kazusa DNA Research Institute (Kisarazu, Chiba, Japan).[26] (AB463134.1) was subcloned into the α-cardiac pJRCATX plasmid carrying the *Myh6* (αMyh) promoter, which was kindly provided by Jeffrey Robbins.[27] This previously described plasmid promotes expression of transgenes in a cardiomyocyte-specific manner. This promoter contains the last exon of the mouse *Myh7* gene, the intergenic region and the first 3 non-coding exons of the *Myh6* gene. There has been a report that the human MYH7b gene encodes a 42 amino acid extension not found in any other MYH7b genes, and therefore, this extension was not included in the transgene. Downstream of the *MYH7b* coding sequence, the Human Growth Hormone gene terminator was used. Even though there is no endogenous MYH7b protein in the mammalian heart,[6] to ensure detection of exogenous MYH7b, the last 10 amino acids of the MYH7b sequence (RDALGPKHKE) were replaced with a c-MYC tag (EQKLISEEDL). The addition of c-MYC has previously been shown to have no effect on full length cardiac myosin in transgenic mouse hearts.[28] This plasmid was then used to generate MYH7b transgenic mice at the University of Colorado, Boulder Transgenic Mouse Facility through microinjection of linearized, purified DNA. Two separate founder mice (F_0) were generated and these were maintained by backcrossing with C57Bl6 (Jackson Laboratories, Bar Harbor, ME). Most experiments described in this study were completed with F3/F4 generations. All experiments were performed with aged-matched, non-transgenic (NTG) littermates, and both sexes were analyzed. None of the experiments described combined sexes. All animal procedures were approved by the University of Colorado, Boulder, CO, Institutional Animal Care and Use Committee, animal protocol number 235116FEB2019.

Genotyping MYH7b Transgenic Mice

Genomic DNA was isolating using the “Quick DNA Purification Protocol” from Jackson Laboratories (www.jax.org). Isolated genomic DNA was then analyzed for the presence of the transgene using primers (forward 5′ AAG GAG CAG GAC ACA AGT GC, reverse 5′ GAA CAG AAG TTG ATC TCT GAA GAA GAT CTG). The GoTaq Green Master Mix (Promega, Madison, WI, USA) was used for transgene amplification with the following cycling conditions: initial denaturation, 94°C for 2 minutes; annealing/elongation, 68°C for 3 minutes; denaturation, 94°C for 15 seconds; cycling a total of 35 times between annealing/elongation and denaturation steps. Transgenic mice were identified by the presence of a 492 bp band on a 2% agarose gel.

Genotyping MYH7b Null Mice

Isolation of genomic DNA

Genomic DNA was isolated as described above. Tail snips were taken from 21-day-old mice and added to 75 μL of 25 mmol/L NaOH+0.2 mmol/L EDTA solution. Reactions were boiled at 99°C for 30 minutes and then cooled to room temperature. 40 mmol/L Tris-HCl was added to the tubes, which were briefly vortexed and then centrifuged. This solution was stored long term at −20°C and 1 μL was used for genotyping.

Genotyping polymerase chain reaction

The isolated genomic DNA was analyzed using Sigma Taq DNA Polymerase from Thermus aquaticus (product number D4545). The following primer pairs were used for genotyping (mMYH7b_forward 5′ TGC TCT TAT GTC TGG AGG TGT and mMYH7b_reverse 5′ GGT AGC AGG CTG ATT CTC C or polyA-reverse 5′ TCC ACT AGT TCT AGA GCG GC). Thermocycling conditions were: 95°C for 15 seconds followed by 33 cycles: 95°C for 15 seconds, 58°C for 15 seconds, 72°C for 30 seconds followed by a final extension at 72°C for 10 minutes. Polymerase chain reaction (PCR) products from each reaction were analyzed by 1% agarose gel. MYH7b null mice were identified by the presence of a band at 218 bp, and wild-type mice were identified by the presence of a band at 242 bp.

SDS-Polyacrylamide Gel Electrophoresis for Separation of Cardiac Myosin Heavy Chain Isoforms

Sample preparation

Frozen left ventricular tissue samples were homogenized and solubilized in Urea-Thiourea sample buffer[29] at the ratio of 1:10. The homogenates were left on a refrigerated rotator for myosin isoform extraction. Samples were vortexed, centrifuged at 19 275*g* for 8 minutes under refrigerated conditions. The supernatant was collected and aliquots frozen and stored at −80°C. Protein concentration was determined using Pierce 660 nm reagent (ThermoFisher).

Before gel loading, samples were thawed, heated for 4 minutes at 55°C, vortexed, and centrifuged at maximum speed for a minute.

Gel preparation and electrophoresis

Gel preparation and electrophoresis conditions were prepared according to the methods previously described by Warren and Greaser.[29] The glass plates that were used were 18×16 cm. A SE600 Hoefer gel system was used with 0.75 mm gel-spacers. Samples were loaded onto 8% polyacrylamide–N,N′-diallyltartardiamide (DATD) gels. The gels were run at 100 V (constant voltage) at 4°C for 25 hours. After electrophoresis, the gels were transferred to gel boxes and fixed with a solution of 50% methanol, 10% acetic acid, for an hour. The gels were rinsed for 10 minutes with MilliQ water and stained overnight with Sypro Ruby Red (Invitrogen). Destaining of the gels was performed using a solution containing 10% methanol and 7% acetic acid. The gels were given 2 rinses 5 minutes each in MilliQ water. The percentages of the MYH isoform bands were determined by densitometry using an LAS scanner.

Echocardiography

Echocardiography analysis was performed as previously described.[30] Briefly, echocardiographic images were taken and measurements were made using a Phillips Sonos 5500 system. Anesthetized mice were placed on a recirculating heating pad maintained at 37°C. Hair was removed from the chest using depilatory cream before the image potentiating gel application. M-mode images were captured for each animal at the level of the papillary muscle (A2 view). Left ventricular dimensions, including functional analysis, was measured using the American Society of Echocardiography (ASE) leading edge convention.

Necropsy and Histological Analysis

Total body weight was collected for each mouse just before euthanasia. Cardiac tissue, including all major vessels, was removed in fully anesthetized mice. Connective tissue was removed, the heart was cannulated through the aorta with sterile saline, and the cleared heart was blotted. The total heart was weighed, the atria were removed and weighed, the right ventricle was separated from the LV, and both ventricles were weighed separately. The tibia was isolated from each mouse and measured to normalize tissue weights. For histological analysis, midline sections from the ventricle were isolated from hearts perfused with 4% paraformaldehyde. Fixed tissue sections were then sent to Premier Laboratories (Longmont, CO) to be embedded in paraffin, sectioned, and stained with hematoxylin and eosin.

Immunofluorescence Analysis

Staining for MYH7b protein was performed on a 10-μm-thick transverse ventricular cryosection taken from a 3-month-old female transgenic mouse. Glass slides were washed once with room temperature PBS for 10 minutes and then incubated with MYH7b antibody[6] diluted 1:50 in PBS for 1 hour 15 minutes at 37°C. Slides were then washed 3 times for 5 minutes with room temperature PBS and incubated with secondary antibody diluted 1:200 in PBS for 1 hour at 37°C (Rhod Red-X-AffiniPure Donkey Anti-Rabbit IgG [H+L], Jackson ImmunoResearch #711-295-152). Finally, slides were washed 3 times for 5 minutes with room temperature PBS and mounted with Fluoromount-G. The imaging work was performed at the BioFrontiers Institute Advanced Light Microscopy Core. Spinning disc confocal microscopy was performed on Nikon Ti-E microscope supported by the BioFrontiers Institute and the Howard Hughes Medical Institute. The whole ventricular section (left panel) was taken on the mCherry channel (594 nm) with a Plan Apo λ 10× optic for 1 second exposure. The right panel image was taken with a Plan Apo λ 40× Ph2 DM optic with a 200 ms exposure.

Electron Microscopy

Isolated hearts were cannulated and perfused with a 0.1 mol/L cacodylate buffer, pH7.4, containing 2.5% glutaraldehyde and 2% paraformaldehyde for a total of 7 minutes. Small sections (≈2 mm square) of the left ventricular free wall were dissected from the fixed tissue and placed in the same buffer/fixative for another 24 hours at 4°C. Further processing was conducted at the electron microscopy core at the University of Colorado, Aurora, CO. After fixation, the small tissue section was rinsed in 100 mmol/L cacodylate buffer and then immersed in 1% osmium and 1.5% potassium ferrocyanide for 15 minutes. Next, the tissue was rinsed 5 times in cacodylate buffer, immersed in 1% osmium for 1 hour, and then rinsed again 5 times for 2 minutes each in cacodylate buffer and 2 times briefly in water. The tissue was transferred to graded ethanol (50%, 70%, 90%, and 100%) containing 2% uranyl acetate for 15 minutes each. Finally, the tissue was transferred through propylene oxide at room temperature and then embedded in LX112 and cured for 48 hours at 60°C in an oven.

Ultra-thin sections (65 nm) were cut on a Reichert Ultracut S from a small trapezoid positioned over the tissue and were picked up on Formvar-coated slot grids (Electron Microscopy Sciences, Hatfield, PA). Sections were imaged on a FEI Tecnai G2 transmission electron microscope (Hillsboro, OR) with an AMT digital camera (Woburn, MA).

Morphological Analysis of Mitochondria

Mitochondrial shape descriptors and size measurements were obtained using Image J (version 1.52i, National Institutes of Health, Bethesda, MD) by manually tracing only clearly discernible outlines mitochondria on electron microscopy images. Surface area (mitochondrial size) is reported in squared pixels; perimeter in pixel; aspect ratio is computed as [(major axis)/(minor axis)] and reflects the "length-to-width ratio"; circularity [4π(surface area/perimeter^2)] and roundness [4(surface area)/(π·major axis^2)] are 2-dimensional indices of sphericity with values of 1 indicating perfect spheroids. Computed values were imported into Origin 2018b (Origin Lab Corporation) for data analysis. To produce frequency distributions of area and roundness, each mitochondrion was assigned to 1 of 12 or 10 bins, respectively, of equal sizes and proportions were determined, yielding frequency histograms, and level of skewness. Skewness is a measure of asymmetry in distributions. A value of 0=normally distributed population.

RNA Extraction

Tissue samples were homogenized in TRI reagent (Molecular Research Center, Cincinnati, OH) and the aqueous phase was separated and isolated using 1/5 volume of chloroform followed by centrifugation at 12 000*g* for 15 minutes. RNA was precipitated with 100% isopropanol and washed with 75% ethanol. RNA pellets were dissolved in HPLC grade water (Sigma Aldrich) and RNA concentrations were determined using a NanoDrop 2000c Spectrophotometer (Thermo Fisher, Waltham, MA).

Quantitative Polymerase Chain Reaction Analysis

RNA at 0.5 to 2.0 μg was reverse transcribed into cDNA using the SuperScript III First-Strand kit (Thermo Fisher/Invitrogen). Real time quantitative polymerase chain reaction (qPCR) was preformed using SYBR Green PCR Master Mix (Thermo Fisher/Applied Biosystems) and the CFX96 Real-Time PCR Detection System (Bio-Rad, Hercules, CA). Primer sequences are listed in Table 1.

Table 1. Summary of qPCR Primer Sequences

Mouse Primer	Primer Sequence
18S (forward)	GCCGCTAGAGGTGAAATTCTTG
18S (reverse)	CTTTCGCTCTGGTCCGTCTT
ANF (forward)	CCAGGCCATATTGGAGCAAA
ANF (reverse)	GAAGCTGTTGCAGCCTAGTC
BNP (forward)	AAGGTGCTGTCCCAGATG
BNP (reverse)	TTGGTCCTTCAAGAGCTGTC
ACTA1 (forward)	CGACATCAGGAAGGACCTGTATGCC
ACTA1 (reverse)	AGCCTCGTCGTACTCCTGCTTGG
MHC-β (forward)	TTCCTTACTTGCTACCCTC
MHC-β (reverse)	CTTCTCAGACTTCCGCAG
MHC-α (forward)	ACATTCTTCAGGATTCTCTG
MHC-α (reverse)	CTCCTTGTCATCAGGCAC
COL1A1 (forward)	AATGGCACGGCTGTGTGCGA
COL1A1 (reverse)	AACGGGTCCCCTTGGGCCTT
CD36 (forward)	GATGTGGAACCCATAACTGGATTCAC
CD36 (reverse)	GGTCCCAGTCTCATTTAGCCACAGT
FATP1 (forward)	ACAGCCAGTTGGACCCTAACTCAA
FATP1 (reverse)	TGGATCTTGAAGGTGCCTGTGGTA
FABP3 (forward)	AACGGGCAGGAGACAACACTAACT
FABP3 (reverse)	TCATAAGTCCGAGTGCTCACCACA
CPT1b (forward)	TTCCGGGACAAAGGCAAGT
CPT1b (reverse)	GCGGTACATGTTTTGGTGCTT
CPT2 (forward)	ACCCTGCCAGAAGTGACAC
CPT2 (reverse)	ACGAGTTGAATTGAAAAGCCGAA
PKCα (forward)	AGAGGTGCCATGAGTTCGTTA
PKCα (reverse)	GGCTTCCGTATGTGTGGATTTT
PKCγ (forward)	AAGTTCACCGCTCGTTTCTC
PKCγ (reverse)	GCTACAGACTTGACATTGCAGG
PKCδ (forward)	AACCGTCGTGGAGCCATTAAA
PKCδ (reverse)	GGCGATAAACTCGTGGTTCTTG
MYH7b MCK genotyping (forward)	ACCAACCTGGCCAAGTAT
MYH7b MCK genotyping (reverse)	CAGAGATCAACTTCTGTTCGG

qPCR indicates quantitative polymerase chain reaction.

Total Protein Extraction

Total cardiac protein lysates were prepared from flash frozen left ventricular tissue. A mortar and pestle, cooled with liquid nitrogen, was first used to grind the tissue into a fine powder. The pulverized tissue was then added to a modified RIPA buffer (1% Nonidet P-40, 0.5% sodium deoxycholate, 0.1% SDS, 1 mmol/L EDTA, 5 mmol/L N-ethylmaleimide, 50 mmol/L sodium fluoride, 2 mmol/L β-glycerophosphate, 1 mmol/L sodium orthovanadate, 100 nmol/L okadaic acid, 5 nmol/L microcystin LR, and 20 mmol/L Tris-HCl, pH 7.6) in which the Halt Protease and Phosphatase Inhibitor Cocktail (100×) (Thermo Fisher, Waltham, MA) was added just before the beginning of the homogenization procedure. Each sample was subjected to mechanical homogenization with a IKAT10 Basic Disperser set at 10 000 rpm for 1 to 2 minutes. Lysates were rocked at 4°C, on an end-over-end rotator, overnight. Lysates were clarified the following morning by

centrifugation at 15 000*g*, at for 4°C, for 15 minutes. After clarification, additional Halt Protease and Phosphatase Inhibitor Cocktail was added and tissue lysates were stored at −80°C until analysis.

Soluble and Myofibril Protein Preparation

Flash frozen ventricular tissue was first pulverized with a mortar and pestle as described above with the exception that the tissue powder was added to 1 mL of K60 buffer (60 mmol/L potassium chloride, 20 mmol/L MOPS [pH 7.0], 2 mmol/L magnesium chloride) in which the Halt Protease and Phosphatase Inhibitor Cocktail (100×) (Thermo Fisher) had been added. Samples were homogenized with a IKAT10 Basic Disperser at 10 000 rpm for 4 to 5 minutes and centrifuged at 15 000*g*, at for 4°C, for 15 minutes. The supernatant was removed and this was label "soluble fraction" for each heart analyzed. The pellet was dispersed by homogenization in 4 mL of K60 buffer (containing protease and phosphatase inhibitors) using a IKAT10 Basic Disperser set at 8000 rpm for 3 to 4 minutes followed by a 10 minute centrifugation, at 3000*g*, set at 4°C. The resultant pellet was homogenized again (3000 rpm for 3–4 minutes) in 4 mL of K60 to which protease and phosphatase inhibitors were added in addition to ethylene glycol-bis(β-aminoethyl ether)-N,N,N′,N′-tetraacetic acid (EGTA, pH 7.0) reaching a final concentration of 1 mmol/L. The homogenate was then centrifuged at 3000*g*, at 4°C, for 10 minutes. The supernatant was again removed and the pellet was once again homogenized using the above described K60-EGTA buffer (containing protease and phosphatase inhibitors) with Triton X-100 added to a final concentration of 1% (4 mL/pellet). Each pellet was homogenized with the IKAT10 Basic Disperser set at 3000 rpm for 30 seconds. Samples were then incubated on ice for 1 hour. Every 10 minutes, each pellet was re-dispersed through homogenization at 5000 rpm for 30 seconds. After 1 hour, homogenates were clarified by a 10 minute centrifugation at 3000*g*, at 4°C. The Triton extraction was repeated once more on the resultant pellet. Each resultant pellet, which was white in color, was gently dispersed in 4 mL of K60 buffer (with only protease and phosphatase inhibitors added) at 756*g* for 30 seconds. This homogenate was centrifuged at 3000*g*, at 4°C, for 10 minutes. This homogenization was repeated one additional time followed by centrifugation at 12 100*g*, at 4°C, for 10 minutes. The final, myofibril fraction, pellet was resuspended in 0.5 mL K60 buffer (with only protease and phosphatase inhibitors added), and the protein concentration was determined using the Pierce BCA Protein Assay kit (Thermo Fisher) protein assay. Myofibrils were diluted to a final concentration of 2 mg/mL in K60 buffer.

Immunoblot Analysis

Protein concentrations were quantitated using the DC Protein Assay (Bio-Rad, Hercules, CA). Equal concentrations of protein were resolved by SDS-Page using 4% to 12% NuPAGE Novex 4% to 12% Bis-Tris Protein Gels and MES SDS Running Buffer (Thermo Fisher). Proteins were either stained with Coomassie blue to visualize total protein or transferred to nitrocellulose membranes (Millipore Corp., Billerica, MA) for immunoblot analysis. For immunoblot analysis, membranes were blocked with 5% blotto for 1 hour at room temperature and incubated with primary antibodies at 4°C, on a shaker, overnight. Primary antibodies included: Cell Signaling[31]: (p38: #9212 Pp38: #4511 ERK: 9102 pERK: 9101), Developmental Hybridoma Bank[32]: (anti-myc tag: 9E10, anti-MyHC: F59), (anti-α Myosin heavy chain: BA-G5), (anti-α-Sarcomeric Actin: mouse IgM isotype, clone 5C5, Sigma #A2172), (anti-β Myosin Heavy Chain mouse monoclonal IgG1, Vector Laboratories #VP-M667). Secondary Antibodies for cell signaling blots: HRP-goat anti rabbit, Jackson cat# 115-035-114 for Developmental hybridoma bank blots: HRP-goat anti mouse, Jackson cat# 115-035-003, #115-035-020 for sarcomeric actin. Blots were developed using Western Lightning Plus Chemiluminescence Substrate (Perkin Elmer) and an ImageQuant LAS 4000 (GE).

Statistical Analysis

Graphpad Prism 7.0 was used to perform all statistical analysis. Unless otherwise stated, all data are represented as ±SEM. Statistical analysis was performed using 2-tailed Student *t* test or 1-way ANOVA with Bonferroni correction post hoc where appropriate. A $P \leq 0.05$ was considered to be statistically significant.

Adult Mouse Ventricular Myocyte Isolation

Adult mouse ventricular myocytes were isolated from the LV of 1.5-month-old mice using a retrograde Langendorff perfusion system and enzymatic digestion (0.1 mg/mL Liberase TM, Sigma-Aldrich), as previously described (Crocini et al[33]). Cells were gradually readapted to calcium by adding 50 or 100 μmol/L $CaCl_2$ every 5 to 8 minutes, until a concentration of 500 μmol/L $CaCl_2$ was reached.

Cardiac Myocyte Contractility Assay and Analysis

Approximately 200 μL of adult mouse ventricular myocyte suspension (≈2500–3000 adult mouse ventricular myocytes/mL) were added onto a 25-mm coverslip inserted in a chamber system (IonOptix, Westwood, MA) and allowed to settle for 5 minutes, before the beginning of the contractility experiment. The chamber system was then transferred to the microscope

(Nikon Diaphot) and superfused in Tyrode buffer (in mmol/L): 113 NaCl, 4.7 KCl, 1.2 $MgCl_2$, 10 glucose, and 10 HEPES; pH adjusted to 7.35 with NaOH. Myocytes were electrically paced via field stimulation at room temperature by using the IonOptix MyoPacer with a stimulus duration of 4 ms, voltage of 1.2× stimulation threshold. The experimental protocol consisted of 0.2, 0.5, 1, 2, 3, 4 Hz of stimulation frequencies. Sarcomere shortening was recorded by IonWizard software (IonOptix, Westwood, MA). At each frequency, 10 contractions per cell were averaged and analyzed. The following parameters were used: sarcomere shortening (%), time-to-peak of contractility (ms), relaxation time at 90% (ms). Within the same sex group, α-MYH7b animals were compared with NTG using ordinary 2-way ANOVA analysis. Frequency of stimulation and genotype were considered the 2 independent variables in the test. A P value of ≤ 0.05 was considered to be statistically significant and was reported for comparison of the mean differences between the genotypes (α-MYH7b and NTG animals).

Results

MYH7b Null Mice Do Not Exhibit a Cardiac Phenotype at Baseline

To determine whether MYH7b plays an important role during cardiac embryogenesis, we monitored the ratio of exon 7 inclusion/skipping during mouse development. We did not detect any increase in exon 7 inclusion during heart development confirming that even though the gene is actively transcribed, the majority of the MYH7b mRNA is not competent for protein production at any stage of mouse heart development (Figure S1). To expand this first observation, we then examined MYH7b null mice created by insertion of 2 transcription terminators after the first exon of the gene (courtesy of E. Olson, UT Southwestern); this configuration also blocks production of the intronic miR-499. Since serious defects in embryonic heart development should be associated with non-Mendelian inheritance, the finding that null litters had the expected ratio of genotypes, suggests that the lack of MYH7B has no detrimental effects on cardiac development (Table S1). We next examined adult MYH7b null mice and found no changes in cardiac mass (Figure 1A); however, while there was no effect on cardiac function in males, we observed a slight enhancement of function in female animals (Figure 1B). Moreover, we measured the expression of 3 canonical markers of cardiac pathology, atrial natriuretic factor (ANF), BNP, and α-skeletal actin and found no significant changes in their expression in left ventricles (LV) isolated from 1.5-month-old mice compared with NTG littermates (Figure 1C). Taken together, these results suggest that MYH7b null mice do not have any obvious baseline cardiac phenotype and therefore MYH7b protein is not required for heart development or function in the adult heart at baseline.

Transgenic Expression of MYH7b in the Mouse Heart

MYH7b protein production in mammals has been inactivated in all but specialized muscles and muscle spindles whereas it is expressed in bird and snake hearts and skeletal muscles (L.A. Leinwand, PhD, unpublished observations, 2019).[6] Thus, we hypothesized that its expression in the mammalian heart would be detrimental because of this evolutionary inactivation. To test this hypothesis, we generated transgenic mice expressing the full-length MYH7b cDNA, which escapes the alternative splicing event that promotes exon 7 skipping. The transgene was placed under the control of the rat α-cardiac myosin promoter that is active only in cardiac myocytes.[27] For unambiguous detection of the transgene protein, we also substituted the last 10 amino acids of the MYH7b amino acid sequence (RDALGPKHKE) with the Myc tag (EQKLISEEDL), which has been found to have no significant functional effect on myosin or other sarcomeric proteins in the mouse heart.[28] Two founders were generated and both of them showed expression of MYH7b by Western blot and myosin separating gels. However, since the total amount of MYH7b produced by one of the founders was extremely low, we performed our analyses only on the line showing expression levels of ≈30% of the total cardiac myosin (Figure 2A). Western blotting with an anti-Myc antibody showed the specificity to detect only the transgenic MYH7b (Figure S2). Because we are interested in sex differences in the heart, we measured MYH7b expression in both sexes and found that equivalent transgene expression was seen in both male and female hearts (data not shown). To determine whether MYH7b was efficiently incorporated into sarcomeres, we next performed fractionation analysis of myofibrillar components and corresponding soluble fractions. The results of this analysis clearly show that MYH7b is incorporated into myofibrils to the same extent as endogenous myosins; more importantly, no accumulation of the transgene was detected in the soluble fraction (Figure 2B through 2D). It is important to note that myosin protein stoichiometry is maintained in transgenic models.[34] Thus, MYH7b myosin replaces corresponding amounts of the endogenous myosins. Immunohistochemical staining of cardiac sections of MYH7b mice with and anti-MYH7b antibody, showed homogeneous distribution of the transgene throughout the heart and higher magnification imaging confirmed sarcomeric incorporation of the MYH7b protein (Figure 2E and 2F).

Expression of MYH7b in the Mouse Heart Results in Sex-Specific Ventricular Mass Increases, Dilation, and Cardiac Dysfunction

We analyzed cardiac morphometry in mice at different time points and found that while both male and female transgenic

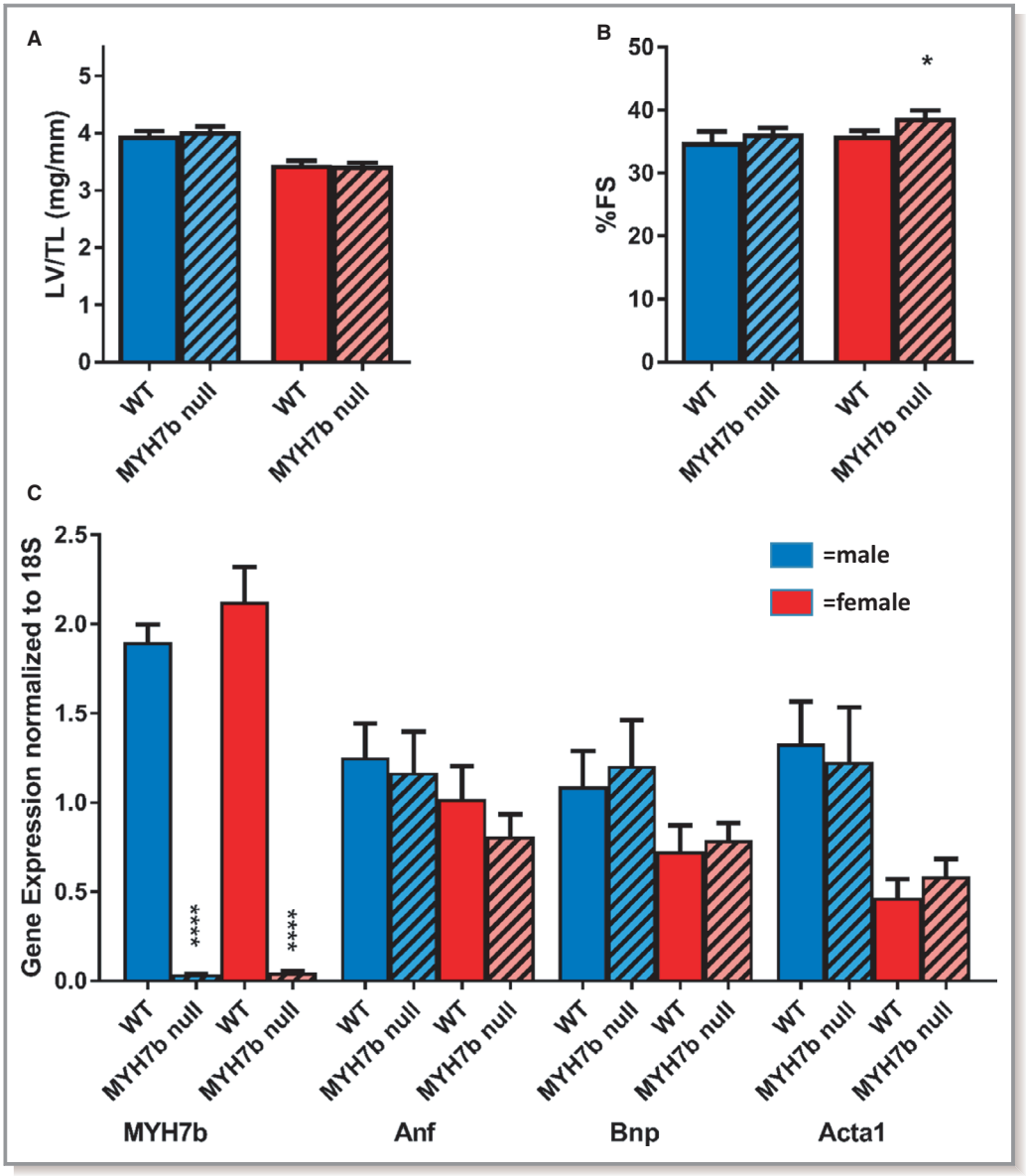

Figure 1. There is no baseline cardiac phenotype in young global-MYH7b null mice. **A**, Left ventricular weights normalized to tibia length (LV/TL mg/mm) show no gross morphometric differences between WT and global-MYH7b null (MYH7b null) in either male or female mice at 1.5 months of age. Animal numbers: male WT n=8, male MYH7b null n=20, female WT n=16, female MYH7b null n=12. **B**, Cardiac contractility as measured by percentage of fractional shortening (%FS) shows cardiac contractility is unaffected in MYH7b null males and slightly enhanced in MYH7b null females. Animal numbers are the same as reported in (**A**). **C**, Gene expression profiling by reverse transcriptase quantitative polymerase chain reaction (RT-qPCR) shows no increases in markers of cardiac pathology in MYH7b null left ventricular tissue. %FS indicates percentage of fractional shortening; LV indicates left ventricle; NTG, non-transgenic; TL, tibial length; WT, wild type. *P value of ≤0.05 by Student t-test. Animal numbers: male WT, n=8; male MYH7b null, n=10; female WT, n=10; female MYH7b null, n=9.

mice have increased LV mass at 1.5 months old, only females show right ventricular mass increases; no changes in atrial mass were observed. (Figure 3A). At 18 months of age, the LV mass increase was still present in both males and female animals, as well as right ventricular mass increase in females, this time also associated with atrial mass increases (Figure 4A). Notably, transgenic male hearts showed significant dilation at both 1.5 and 18 months of age whereas female hearts were dilated only at 18 months as viewed in cross-sections (Figures 3B and 4B). Cardiac function was assessed by echocardiography and fractional shortening was significantly decreased at 3, 6, 12, and 18 months in α-

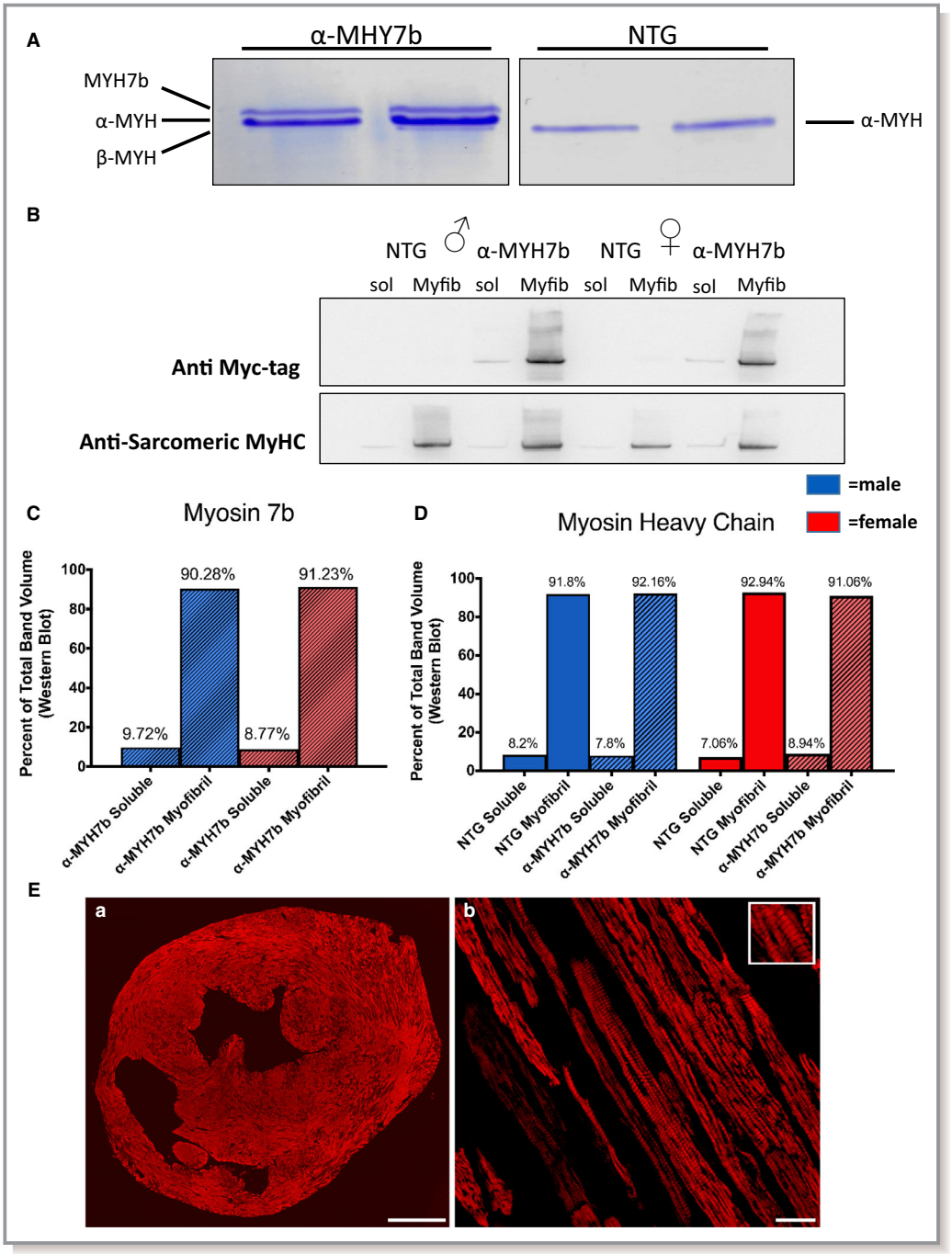

Figure 2. MYH7b is expressed in mouse hearts and is incorporated into sarcomeres. **A**, Myosin separating gel showing transgenic protein expression from 2 separate female mice (2 months of age) for both NTG and α-MYH7b transgenic mice. Transgene expression was ≈30% of the total myosin in the α-MYH7b LV compared with NTG controls. **B**, Western blot analysis of myofibril isolation preps from both male and female 1.5-month-old mice showing exogenously expressed MYH7b (Myc-tag, upper blot) is incorporated into intact myofibrils to the same extent as endogenously expressed myosin (Anti-Sarcomeric MyHC, lower blot). **C** and **D**, Quantitation of both exogenous and endogenous myosin incorporation into intact myofibrils. Results are shown as proportion of each myosin relative to the total myosin in each fraction. **E**, (**a**) Immunofluorescence image of a transverse cross section of the LV and right ventricle (RV) showing abundant and widespread distribution of the MYH7b protein; scale bar=1 mm. (**b**) Higher magnification figure showing incorporation of MYH7b into sarcomeres as evidenced by the striated pattern. Inset box shows higher magnification of the sarcomere; scale bar=20 μm. Samples were stained using an antibody directed against the MYH7b protein. MyFib indicates myofibril fraction; sol, soluble fraction; Myc, c-myc tag; MyHC, myosin heavy chain.

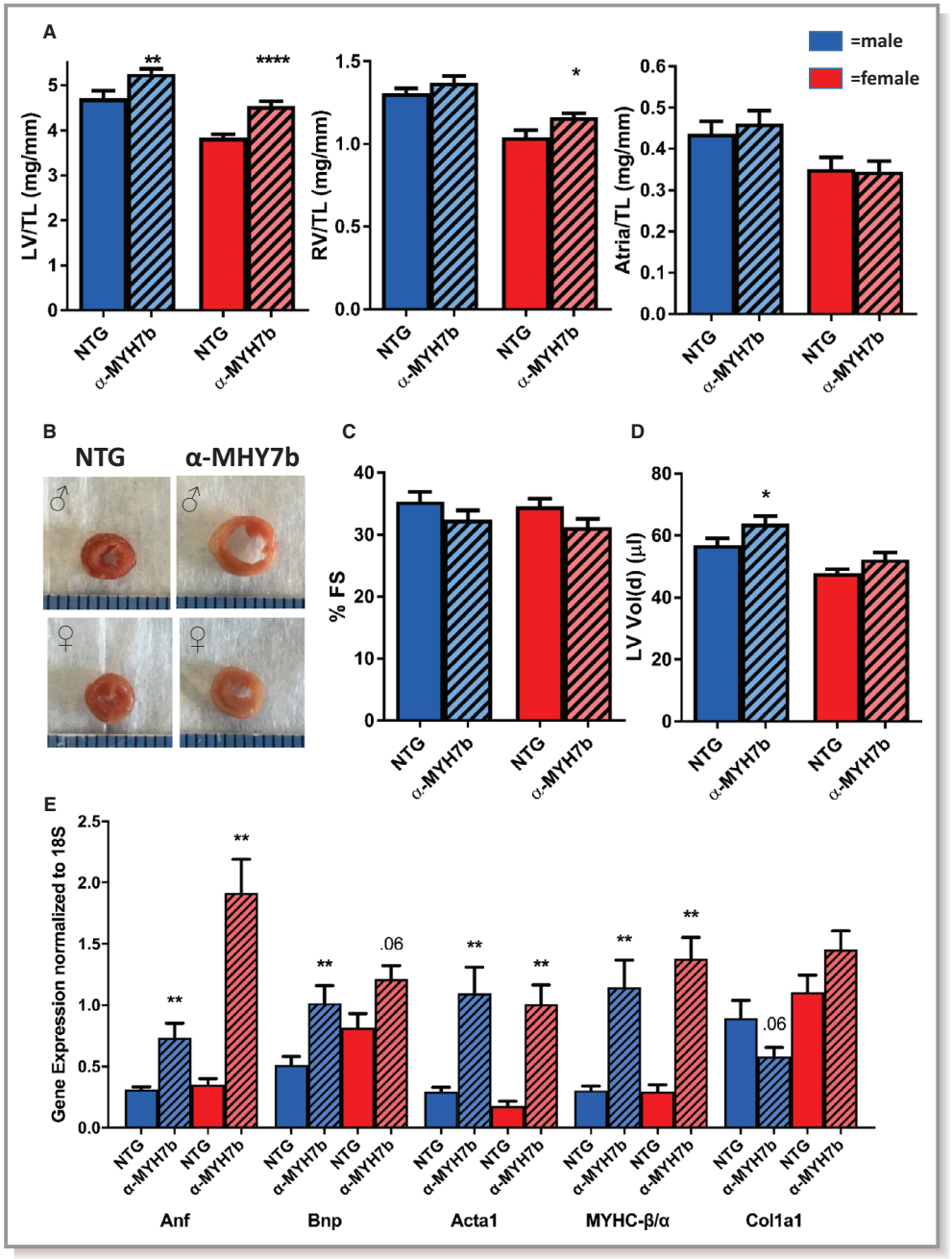

Figure 3. MYH7b expression results in morphometric changes in 1.5-month-old mice. **A**, Morphological measurements comparing LV, RV, and atrial weights normalized to tibial length in male and female NTG and α-MHY7b mice at 1.5 months of age. **B**, Gross morphological images of ventricular cross sections of male and female NTG and α-MYH7b transgenic mice confirm the presence of cardiac dilation in male α-MHY7b mice. **C** and **D**, Echocardiographic profiles of young 1.5-month-old male and female mice show no significant functional changes (%FS) but early cardiac dilation (LV Vol(d) μL) in male α-MYH7b mice. **E**, Gene expression analysis showing increased expression of fetal genes in both male and female α-MYH7b transgenic mice at 1.5 months. %FS indicates percentage of fractional shortening; LV indicates left ventricle; NTG, non-transgenic; TL, tibial length. **P*≤0.05; ***P*≤0.01, ****P*≤0.001, *****P*≤0.0001. Animal numbers: male NTG, n=13; male α-MYH7b, n=17; female NTG, n=7; female α-MYH7b, n=21.

MYH7b male mice (Figures 3C and 4C; Figure S3). While a significant decline in cardiac contractile function was also noted in female mice, it only reached significance at 12 and 18 months of age (Figures 3C and 4C; Tables 2 and 3). LV chamber dilation was also observed in both sexes but male mice displayed an earlier onset (1.5 months old) indicating

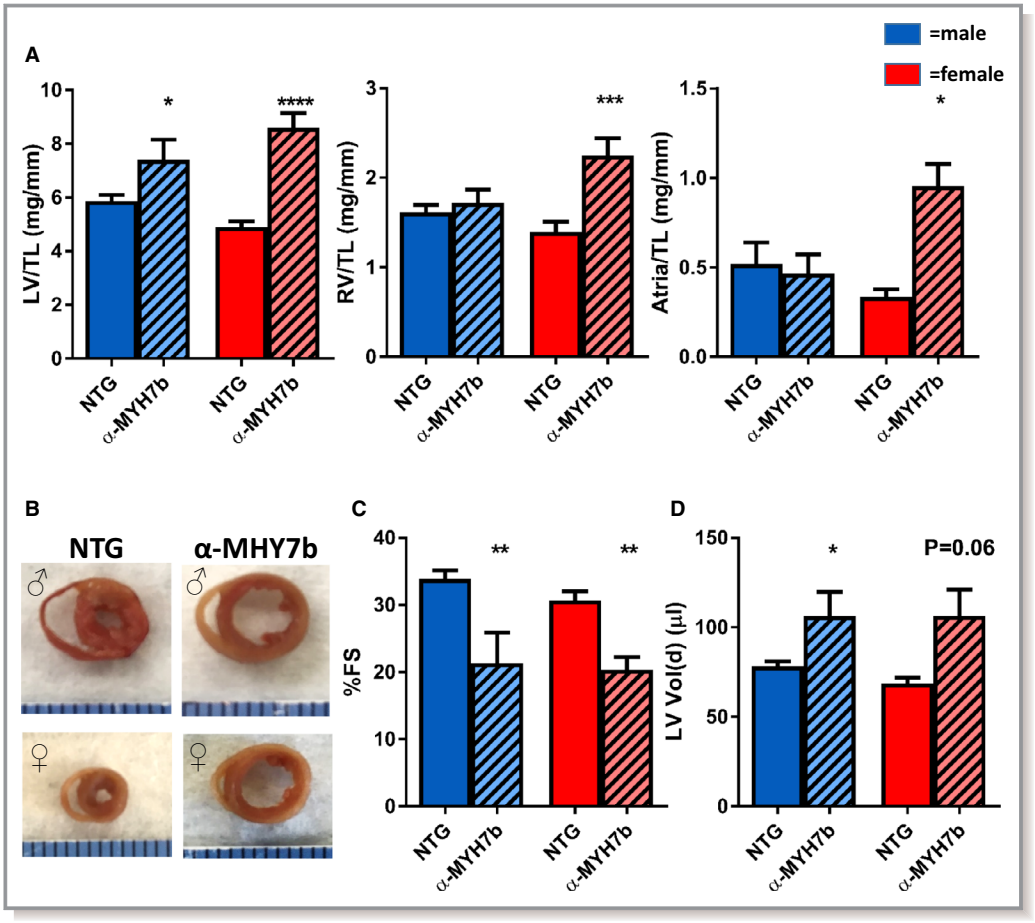

Figure 4. MYH7b expression results in progressive cardiac dilation and LV dysfunction. **A**, Morphological measurements comparing LV, RV, and atrial weights normalized to tibial length (TL) in male and female NTG and α-MHY7b mice. **B**, Gross morphological images of ventricular cross sections of male and female NTG and α-MYH7b mice, confirming presence of cardiac dilation in both sexes by 18 months of age. Echocardiographic profiles of 18-month-old male and female mice showing (**C**) significant functional changes (%FS) and (**D**) cardiac dilation (diastolic left ventricular volume [LV Vol(d)] µL) in both male and female α-MYH7b mice. %FS indicates percentage of fractional shortening; LV indicates left ventricle; NTG, non-transgenic; RV, right ventricle; TL, tibial length. *$P \leq 0.05$; **$P \leq 0.01$, ***$P \leq 0.001$, ****P=0.0001. Animal numbers: male NTG n=12, male α-MYH7b n=6, female NTG n=10, female α-MYH7b n=17.

more chronic, progressive pathology compared with females who only developed dilation at 18 months old (Figures 3D and 4D; Tables 1 and 2).

Since alterations in mitochondrial ultrastructure have been reported in transgenic models of cardiomyopathy,[35] we also performed electron microscopy on heart sections of α-MYH7b animals analyzed at 1.5 and 18 months of age and saw no gross effects on mitochondrial size and shape (Figures S4 and S5). An increased aspect ratio of mitochondria was found in only 1 male mouse at 1.5 months, an indication of more elongated mitochondria. However, both roundness and circularity were unchanged (Figure S4B).

In addition to the morphologic and cardiac function analysis, we also measured the expression of several genes that are induced during heart disease. We found that the expression of many of these markers was induced at 1.5 months of age, before the onset of contractile dysfunction. While many of them were elevated in both sexes, ANF was significantly more induced in female hearts than in male hearts (Figure 3E). Since this is a myosin-induced cardiomyopathy, we also analyzed pathways known to be altered in other transgenic models expressing mutant myosin's. For example, in many cardiomyopathy models, there is a metabolic shift from fatty acid oxidation to glycolysis.[36] Since alteration in the expression of genes change involved in energy consumption use can be indicative of this metabolic shift, we analyzed the levels of expression of CD36, FATP1, FABP3, CPT1 and CPT2 in 1.5-month-old animals (Figure S6) but we did not find any evidence supporting changes in cellular metabolism. Moreover, MAPK signaling through p38 and ERK1/2 also showed no sign of activation (Figures S7 and S8).

Table 2. Echocardiographic Measurements of Male α-MYH7b and NTG Mouse Hearts

	1.5 Months		3 Months		6 Months		9 Months		12 Months		18 Months	
	NTG	α-MYH7b	NTG	α-MYH7b	NTG	α-MYH7b	NTG	α-MYH7b	NTG	α-MYH7b	NTG	α-MYH7b
	n=14	n=15	n=5	n=13	n=20	n=16	n=10	n=13	n=15	n=15	n=12	n=6
LVAW; diastole (cm)	0.066	0.067	0.067	0.069	0.069	0.07	0.07	0.073	0.075	0.075	0.077	0.073
SD	0.002	0.003	0.003	0.002	0.002	0.003	0.002	0.003	0.002	0.003	0.003	0.008
P value		0.637		0.075		0.116		0.003*		0.663		0.144
LVID; diastole (cm)	0.366	0.384	0.396	0.392	0.378	0.438	0.38	0.407	0.389	0.443	0.419	0.473
SD	0.022	0.023	0.015	0.042	0.034	0.108	0.034	0.047	0.022	0.046	0.022	0.063
P value		0.042*		0.858		0.025*		0.123		0.000*		0.015*
LVPW; diastole (cm)	0.067	0.067	0.067	0.069	0.069	0.07	0.073	0.072	0.073	0.074	0.079	0.074
SD	0.003	0.002	0.001	0.002	0.002	0.001	0.002	0.003	0.003	0.003	0.004	0.01
P value		0.64		0.191		0.091		0.12		0.591		0.228
LVAW; systole (cm)	0.106	0.107	0.119	0.109	0.106	0.105	0.108	0.106	0.114	0.108	0.122	0.106
SD	0.008	0.006	0.13	0.012	0.007	0.008	0.009	0.007	0.007	0.008	0.008	0.019
P value		0.478		0.144		0.807		0.719		0.029*		0.023*
LVID; systole (cm)	0.24	0.263	0.246	0.279	0.24	0.328	0.244	0.28	0.253	0.319	0.277	0.375
SD	0.027	0.028	0.033	0.049	0.032	0.12	0.042	0.062	0.024	0.061	0.029	0.089
P value		0.031*		0.182		0.003*		0.121		0.001*		0.003*
LVPW; systole (cm)	0.103	0.105	0.115	0.104	0.11	0.106	0.118	0.116	0.119	0.115	0.121	0.11
SD	0.006	0.006	0.005	0.008	0.005	0.009	0.005	0.011	0.007	0.008	0.006	0.035
P value		0.488		0.014*		0.097		0.723		0.13		0.3*
LV Vol; diastole (μL)	56.932	63.894	68.436	67.941	61.784	93.947	62.809	74.192	65.973	90.256	78.283	106.229
SD	8.423	9.221	5.971	18.268	12.777	68.602	12.715	19.853	9.024	23.039	9.584	33.223
P value		0.044*		0.954		0.047*		0.108		0.001*		0.014*
LV Vol; systole (μL)	20.536	25.759	21.907	30.773	20.791	52.287	22.04	31.781	23.314	42.99	29.361	64.458
SD	5.677	6.47	6.903	14.866	6.999	59.416	8.954	16.637	6.039	19.32	6.948	34.126
P value		0.029*		0.224		0.024*		0.102		0.001*		0.003*
EF (%)	64.449	60.153	68.368	56.303	66.886	51.611	65.736	59.649	64.747	54.176	62.895	41.98
SD	5.427	6.024	8.465	8.693	5.428	12.887	10.328	12.006	6.21	11.13	6.11	18.145
P value		0.054		0.017*		0.000*		0.215		0.003*		0.002*
FS (%)	34.614	31.679	38.07	29.216	36.548	26.565	36.056	31.917	35.046	28.359	33.873	21.365
SD	3.977	4.213	6.643	5.541	4.098	7.511	7.391	8.274	4.473	7.811	4.459	11.054
P value		0.065		0.011*		0.000*		0.223		0.008*		0.003*
HR (bpm)	491.933	495.96	449.937	488.123	466.946	503.276	469.511	479.11	452.742	477.62	465.336	470.921
SD	41.594	38.55	79.581	34.307	58.233	51.285	71.305	44.25	43.362	41.336	36.141	27.481
P value		0.789		0.163		0.058		0.614		0.119		0.744

EF indicates ejection fraction; FS, fractional shortening; HR, heart rate; LVAW, left ventricular anterior wall; LVID, left ventricular internal dimension; LVPW, left ventricular posterior wall; LV Vol, left ventricular volume.
*$P \leq 0.05$.

Table 3. Echocardiographic Measurements of Female α-MYH7b and NTG Mouse Hearts

	1.5 Months		3 Months		6 Months		9 Months		12 Months		18 Months	
	NTG	α-MYH7b	NTG	α-MYH7b	NTG	α-MYH7b	NTG	α-MYH7b	NTG	α-MYH7b	NTG	α-MYH7b
	n=9	n=11	n=9	n=12	n=8	n=17	n=10	n=12	n=12	n=7	n=10	n=17
LVAW; diastole (cm)	0.068	0.065	0.068	0.068	0.069	0.071	0.069	0.070	0.068	0.069	0.080	0.072
SD	0.004	0.003	0.001	0.001	0.002	0.003	0.001	0.001	0.001	0.002	0.006	0.007
P value		0.069		0.546		0.067		0.009*		0.412		0.006*
LVID; diastole (cm)	0.341	0.354	0.357	0.377	0.360	0.363	0.361	0.4378	0.368	0.377	0.396	0.464
SD	0.012	0.020	0.025	0.037	0.011	0.032	0.014	0.031	0.011	0.020	0.025	0.106
P value		0.125		0.184		0.822		0.125		0.216		0.059
LVPW; diastole (cm)	0.069	0.068	0.066	0.068	0.069	0.069	0.069	0.071	0.069	0.070	0.078	0.070
SD	0.003	0.004	0.003	0.003	0.002	0.002	0.001	0.002	0.002	0.003	0.005	0.008
P value		0.559		0.206		0.792		0.009*		0.220		0.212*
LVAW; systole (cm)	0.104	0.098	0.107	0.105	0.110	0.107	0.108	0.107	0.110	0.104	0.120	0.101
SD	0.008	0.008	0.007	0.014	0.003	0.008	0.009	0.007	0.008	0.006	0.010	0.013
P value		0.087		0.706		0.286		0.743		0.089		0.001*
LVID; systole (cm)	0.223	0.243	0.228	0.253	0.226	0.239	0.232	0.249	0.225	0.254	0.278	0.371
SD	0.017	0.008	0.007	0.051	0.017	0.028	0.020	0.043	0.019	0.017	0.020	0.121
P value		0.087		0.706		0.286		0.743		0.089		0.001*
LVPW; systole (cm)	0.102	0.099	0.104	0.109	0.107	0.107	0.109	0.114	0.113	0.109	0.115	0.105
SD	0.006	0.008	0.009	0.012	0.009	0.005	0.005	0.008	0.009	0.007	0.012	0.017
P value		0.388		0.309		0.912		0.094		0.282		0.112
LV Vol; diastole (μL)	47.964	52.383	53.551	61.458	54.551	56.075	54.929	61.707	57.374	60.923	68.713	106.300
SD	3.897	7.2	8.971	15.194	4.034	11.839	5.037	12.808	3.898	7.68	10.68	61.149
P value		0.117		0.182		0.729		0.132		0.195		0.067
LV Vol; systole (μL)	17.000	21.252	17.937	24.482	17.454	20.367	18.653	23.087	17.432	23.347	29.199	67.573
SD	3.345	5.632	4.148	12.618	3.311	5.863	4.123	11.232	3.518	3.726	5.132	54.294
P value		0.062		0.153		0.206		0.252		0.003*		0.036*
EF (%)	64.738	59.846	66.634	61.454	67.948	63.876	66.290	63.834	69.633	61.612	57.426	42.563
SD	4.946	6.394	3.870	13.214	5.71	6.057	4.938	9.619	5.593	4.444	4.916	15.658
P value		0.077		0.271		0.124		0.474		0.005*		0.008*
FS (%)	34.610	31.259	36.104	33.156	37.267	34.196	35.938	34.531	38.700	32.583	29.822	21.437
SD	3.651	4.293	2.920	9.186	4.491	4.355	3.743	6.774	4.716	3.308	3.251	9.259
P value		0.080		0.367		0.117		0.565		0.008*		0.011*
HR (bpm)	493.724	496.586	459.035	445.338	489.308	465.740	501.526	482.845	467.679	457.697	451.609	482.614
SD	38.855	28.994	36.047	43.751	33.048	35.118	39.241	59.421	43.905	38.785	37.083	38.029
P value		0.852		0.455		0.125		0.405		0.625		0.050*

EF indicates ejection fraction; FS, fractional shortening; HR, heart rate; LVAW, left ventricular anterior wall; LVID, left ventricular internal dimension; LVPW, left ventricular posterior wall; LV Vol, left ventricular volume.
*$P \leq 0.05$.

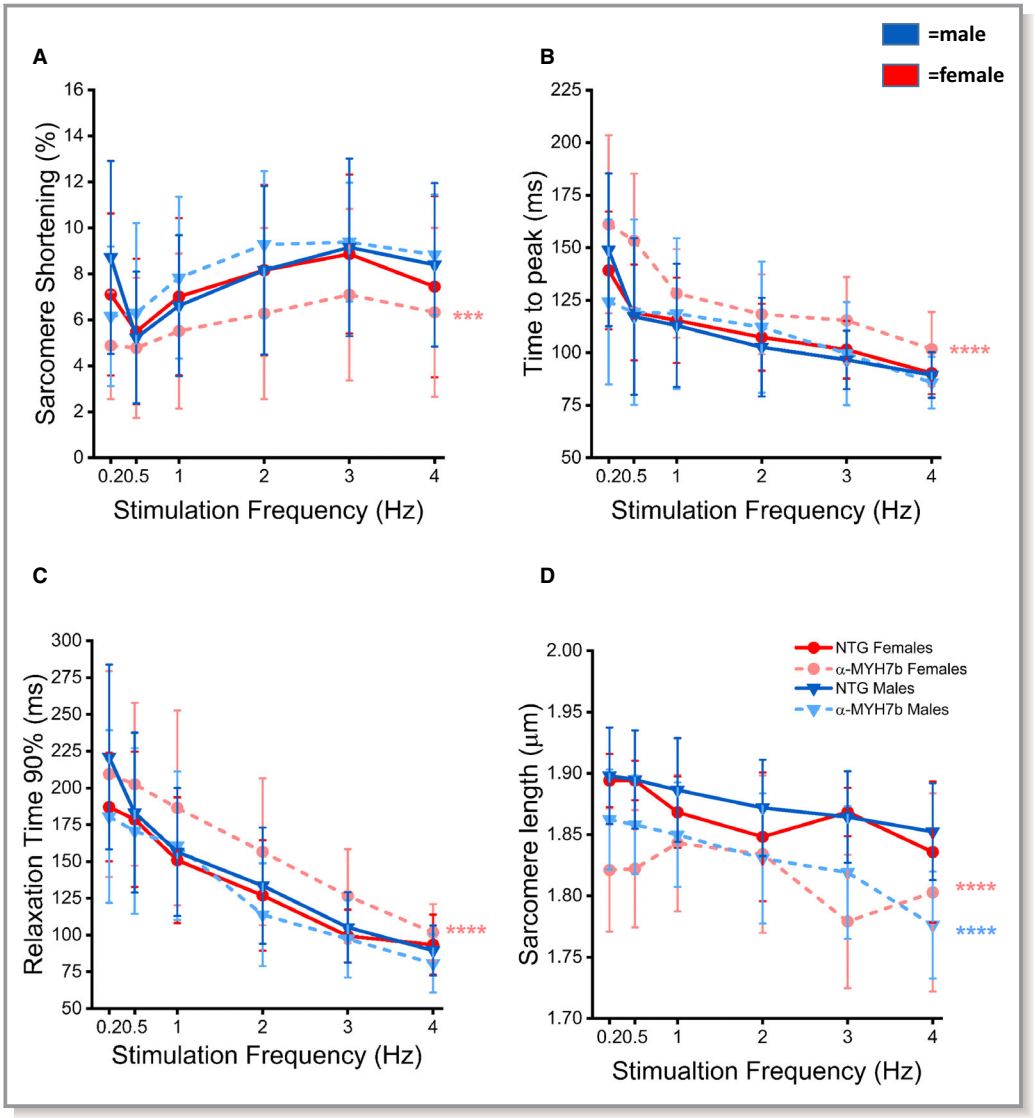

Figure 5. Contractile function in isolated myocytes from 1.5-month-old mice. **A**, Percentage of sarcomere shortening at frequencies ranging from 0.2 to 4 Hz in isolated myocytes from both male and female NTG and α-MYH7b mice. **B**, Time from stimulus to peak contraction and (**C**) time from peak to 90% relaxation at frequencies ranging from 0.2 to 4 Hz in isolated myocytes from both male and female NTG and α-MYH7b transgenic mice. **D**, Sarcomere length (in μm) at frequencies ranging from 0.2 to 4 Hz in isolated myocytes from both male and female NTG and α-MYH7b mice. All measurements were performed at steady-state. Data reported as mean±SD from 16 cardiomyocytes from 4 NTG male mice (blue curves), 21 cardiomyocytes from 5 α-MYH7b male mice (light blue curves), 28 cardiomyocytes from 5 NTG female mice (red curves), and 19 cardiomyocytes from 5 α-MYH7b female mice (pink curves). Data were analyzed using 2-way ANOVA and differences between genotypes are reported in the figure (***$P \leq 0.001$, ****$P \leq 0.0001$). NTG indicates non-transgenic.

Cardiac Myocytes Isolated From 1.5-Month-Old Female α-MYH7b Mice Show Defects in Contractility

To increase the resolution of our analysis and gather molecular insight on the development of the dilated cardiomyopathy, we next isolated cardiomyocytes from α-MYH7b animals and determined their contractile properties at the single cell level. We measured all parameters at steady-state using a range of stimulation frequencies (0.2–4 Hz) to study the shortening-frequency relationship and frequency-dependent acceleration. The shortening-frequency relationship in NTG cardiac myocytes showed the characteristic negative phase at low stimulation frequencies (<1 Hz) and a biphasic response at higher stimulation frequencies (>1 Hz) (Figure 5A), as previously reported for room temperature

measurements.[37] No significant differences of cardiac cell contractility were observed between sexes in NTG animals (Figure 5). As shown in Figure 5, only cells harvested from 1.5-month-old female mice had impaired contractile function: the percentage of sarcomere shortening was decreased, time to peak shortening was slower, and 90% relaxation was slower (Figure 5A through 5C). Interestingly, cardiomyocytes isolated from both male and female mice show reduced sarcomere length at baseline (Figure 5D), supporting the idea that cardiac myofilaments containing Myh7b are pre-activated.

Discussion

In the present study we provide evidence that the MYH7b gene does not play an obvious role in mouse heart development, or in the adult mouse heart at baseline. Further, forced expression of MYH7b protein in the mouse heart causes a severe dilated cardiomyopathy. Numerous studies have reported associations between variants in the human MYH7b gene that are predicted to be pathogenic and a variety of cardiovascular abnormalities, including long QT syndrome, ventricular septal defect, and LVNC among others.[38] These findings have been puzzling since we previously found that in the mammalian heart, MYH7b RNA is not translated because of non-productive splicing of the gene which introduces an early premature termination codon in the transcript.[9] While our results do not shed light on the aforementioned association studies, they do suggest that the MYH7b gene variants linked to heart disease do not operate through the MYH7b protein. Thus, active MYH7b cardiac transcription may be maintained only to ensure production of the intronic microRNA 499 or MYH7b RNA itself may play a regulatory role.

Further, our results clearly demonstrate that MYH7b protein (it should be noted that transgene is the human MYH7b, 97% identical to mouse) expression in the mouse heart is not tolerated despite of the fact that MYH7b protein is expressed in chicken and snake striated muscles. The human and mouse MYH7b genes share substantial homology (≈69% identity for both the motor and rod domains) with α and β-cardiac MyHCs which are the main myosin motors expressed in mammalian hearts.[39] Although the motor domains of the latter 2 myosin's share 93% amino acid identity, their functional properties are distinct.[1] Since we have shown that MYH7b is efficiently incorporated into the sarcomeres of mouse cardiomyocytes, we believe that the amino acid differences found in the motor domains of MYH7b human/mouse versus chicken/snake must confer different motor properties to different vertebrate species. While, for example, the human MYH7b motor domain has evolved to work only in specialized muscles such as extraocular muscles, the chicken homolog can functionally interact with the other myosin isoforms expressed in the heart. We show that when ≈30% of the myosin molecules incorporated into the thick filaments consist MYH7b in the mouse, the contractile function of the heart is pathologically affected. By 1.5 months of age, the MYH7b transgenic mice show increases in LV mass in both males and females, increases in right ventricular mass in females and LV dilation in males. These morphological changes progress to significant decreases in cardiac function in males by 3 months of age. Surprisingly, in females, the morphological changes do not lead to cardiac dysfunction until 12 months of age despite abnormalities in gene expression and myocyte contractility. This finding shows that despite the fact that female α-MYH7b mice show early significant cardiac mass increases, they are protected from cardiac dysfunction and dilation until late adulthood. Previously, we have also reported similar sexual dimorphisms in a myosin mutant model of hypertrophic cardiomyopathy.[40] While originally it was hypothesized that estrogen was protecting female mice from more significant disease in this model, further experiments showed that was not the case, since male animals administered estrogen exhibited mortality.[41]

Both male and female α-MYH7b mice showed significant increases in ANF, α skeletal muscle actin, and the ratio of β-MYH/α-MYH at 1.5 months of age. While trending towards an increase in female mice at this age, male mice displayed significant elevations in BNP. Surprisingly, we did not detect any alterations in the p38 or the ERK signaling pathways in either young or older adult transgenic mice (1.5, 12 months, respectively) or significant increases in Collagen type 1a (Col1a) which is one of the primary components of the cardiac extracellular matrix. Consistent with that observation, we did not identify any sign of fibrosis in the myocardial interstitium (data not shown). Thus, it appears that enlargement of ventricular mass, enlargement of the left-ventricular chamber and cardiac dysfunction are not caused by activation of canonical cardiac pathological signaling pathways. Interestingly, single cell contractile analysis showed that female myocytes had reduced maximal shortening as well as slower kinetics of contraction and relaxation. Moreover, neither sex showed a negative shortening-frequency relationship at low frequencies of stimulation, an indication of a different SR calcium load at a low frequency of stimulation. Additionally, the finding that MYH7b myofilaments could be preactivated suggests that the basal activation of myofilaments under resting conditions could lead to impairment of the relaxation phase in diastole. Hence, our data suggest that Myh7b expression could predominantly affect systolic function at an earlier stage while diastolic dysfunction may arise in older mice because of the reduced sarcomere length observed at rest. Stimulation frequencies more similar to those existing in vivo could unveil a worse contractile phenotype in male cardiomyocytes. In contrast, female mice could be cardioprotected by different mechanisms that counterbalance the mechanical impairment produced by expression of MYH7b.

For example, in female mice, action potential duration is lengthened by reduced expression of Kv1.5 and its corresponding K^+ current, I_{Kur}.[42] Additionally, Ca^{2+} transients, Ca^{2+} sparks, and excitation-contraction coupling gain are lower in female cardiomyocytes[43] and these differences are at least in part mediated by the cAMP/PKA pathway. The integration of all these mechanisms could be responsible for the later functional and structural manifestations observed by echocardiography in α-MYH7b female mice as compared with their male counterparts.

It remains unclear how the forced incorporation of MYH7b in the sarcomeres of α-MYH7b animals activates the first pathological steps that lead to cardiac disease. One possible hypothesis is altered sarcomeric force generation and transmission caused by the enzymatic activity of MYH7b normally operating in concert with other motor isoforms only in specialized muscles. Molecular sensors, such as titin, might then sense the pathological contractile changes and respond by reprogramming nuclear transcription without the involvement of any other signal transduction pathways.[44]

By expanding our knowledge of tissue-specific regulated expression of MYH7b and sarcomeric contractile activity, our data may be useful to better understand the complex functional interplay occurring among different myosin isoforms populating the same sarcomere.

Acknowledgments

The authors would like to thank Dr Eric Olson at UT Southwestern for providing the global MYH7b null mouse line. The authors would also like to thank the Director of the BioFrontiers Imaging Core, Joe Dragavon, and the Director of the Electron Microscopy Core, Jennifer Bourne, for their technical assistance and support. We would like to acknowledge Deepa Puthenvedu at Biofrontiers Institute, University of Colorado, Boulder, CO. for the myosin separating gel.

Sources of Funding

Dr Crocini was supported by the Human Frontiers Science Program Fellowship (LT001449/2017-L). L. A. Lee received grant support from NIH T32 GM008759. Research Grant support was provided by NIH GM029090 to Dr Leinwand.

Disclosures

None.

References

1. Deacon J, Bloemink M, Rezavandi H, Geeves M, Leinwand L. Identification of functional differences between recombinant human α and β cardiac myosin motors. *Cell Mol Life Sci*. 2012;69:2261–2277.
2. Krenz M, Robbins J. Impact of beta-myosin heavy chain expression on cardiac function during stress. *J Am Coll Cardiol*. 2004;44:2390–2397.
3. Krenz M, Sanbe A, Bouyer-Dalloz F, Gulick J, Klevitsky R, Hewett T, Osinska H, Lorenz J, Brosseau C, Federico A, Alpert N, Warshaw D, Perryman M, Helmke S, Robbins J. Analysis of myosin heavy chain functionality in the heart. *J Biol Chem*. 2003;278:17469–17474.
4. Nakao K, Minobe W, Roden R, Bristow M, Leinwand L. Myosin heavy chain gene expression in human heart failure. *J Clin Invest*. 1997;100:2362–2370.
5. Desjardins P, Burkman J, Shrager J, Allmond L, Stedman H. Evolutionary implications of three novel members of the human sarcomeric myosin heavy chain gene family. *Mol Biol Evol*. 2002;19:375–393.
6. Rossi A, Mammucari C, Argenti C, Reggiani C, Schiaffino S. Two novel/ancient myosins in mammalian skeletal muscles: MYH14/7b and MYH15 are expressed in extraocular muscles and muscle spindles. *J Physiol*. 2010;588:353–364.
7. van Rooij E, Quiat D, Johnson B, Sutherland L, Qi X, Richardson J, Kelm RJ, Olson E. A family of microRNAs encoded by myosin genes governs myosin expression and muscle performance. *Dev Cell*. 2009;17:662–673.
8. Wang J, Jiao J, Li Q, Long B, Wang K, Liu J, Li Y, Li P. miR-499 regulates mitochondrial dynamics by targeting calcineurin and dynamin-related protein-1. *Nat Med*. 2011;17:71–78.
9. Bell M, Buvoli M, Leinwand L. Uncoupling of expression of an intronic microRNA and its myosin host gene by exon skipping. *Mol Cell Biol*. 2010;30:1937–1945.
10. Blech-Hermoni Y, Dasgupta T, Coram R, Ladd A. Identification of targets of CUG-BP, Elav-like family member 1 (CELF1) regulation in embryonic heart muscle. *PLoS One*. 2016;11:e0149061.
11. Rakus D, Gizak A, Wiśniewski J. Proteomics unveils fibroblast-cardiomyocyte lactate shuttle and hexokinase paradox in mouse muscles. *J Proteome Res*. 2016;15:2479–2490.
12. Rüdebusch J, Benkner A, Poesch A, Dörr M, Völker U, Grube K, Hammer E, Felix S. Dynamic adaptation of myocardial proteome during heart failure development. *PLoS One*. 2017;12:e0185915.
13. Warkman A, Whitman S, Miller M, Garriock R, Schwach C, Gregorio C, Krieg P. Developmental expression and cardiac transcriptional regulation of Myh7b, a third myosin heavy chain in the vertebrate heart. *Cytoskeleton (Hoboken)*. 2012;69:324–335.
14. Rubio MD, Johnson R, Miller CA, Huganir RL, Rumbaugh G. Regulation of synapse structure and function by distinct myosin II motors. *J Neurosci*. 2011;31:1448–1460.
15. Haraksingh R, Jahanbani F, Rodriguez-Paris J, Gelernter J, Nadeau K, Oghalai J, Schrijver I, Snyder M. Exome sequencing and genome-wide copy number variant mapping reveal novel associations with sensorineural hereditary hearing loss. *BMC Genomics*. 2014;15:1155.
16. Esposito T, Sampaolo S, Limongelli G, Varone A, Formicola D, Diodato D, Farina O, Napolitano F, Pacileo G, Gianfrancesco F, Di Iorio G. Digenic mutational inheritance of the integrin alpha 7 and the myosin heavy chain 7B genes causes congenital myopathy with left ventricular non-compact cardiomyopathy. *Orphanet J Rare Dis*. 2013;8:91.
17. Wu M. Mechanisms of trabecular formation and specification during cardiogenesis. *Pediatr Cardiol*. 2018;39:1082–1089.
18. Anderson RH, Jensen B, Mohun TJ, Petersen SE, Aung N, Zemrak F, Planken RN, MacIver DH. Key questions relating to left ventricular noncompaction cardiomyopathy: is the emperor still wearing any clothes? *Can J Cardiol*. 2017;33:747–757.
19. Rooms I, Dujardin K, De Sutter J. Non-compaction cardiomyopathy: a genetically and clinically heterogeneous disorder. *Acta Cardiol*. 2015;70:625–631.
20. Towbin JA, Lorts A, Jefferies JL. Left ventricular non-compaction cardiomyopathy. *Lancet*. 2015;386:813–825.
21. Zhang W, Chen H, Qu X, Chang CP, Shou W. Molecular mechanism of ventricular trabeculation/compaction and the pathogenesis of the left ventricular noncompaction cardiomyopathy (LVNC). *Am J Med Genet C Semin Med Genet*. 2013;163C:144–156.
22. Val-Bernal JF, Garijo MF, Rodriguez-Villar D, Val D. Non-compaction of the ventricular myocardium: a cardiomyopathy in search of a pathoanatomical definition. *Histol Histopathol*. 2010;25:495–503.
23. Stöllberger C, Wegner C, Finsterer J. Left ventricular hypertrabeculation/noncompaction, cardiac phenotype, and neuromuscular disorders. *Herz*. 2018. Available at: https://link.springer.com/article/10.1007%2Fs00059-018-4695-1. Accessed July 23, 2019.
24. Peselow E, Filippi A, Goodnick P, Barouche F, Fieve R. The short- and long-term efficacy of paroxetine HCl: A. Data from a 6-week double-blind parallel design trial vs. imipramine and placebo. *Psychopharmacol Bull*. 1989;25:267–271.
25. Long C, McAnally J, Shelton J, Mireault A, Bassel-Duby R, Olson E. Prevention of muscular dystrophy in mice by CRISPR/Cas9-mediated editing of germline DNA. *Science*. 2014;345:1184–1188.

26. Nagase T, Yamakawa H, Tadokoro S, Nakajima D, Inoue S, Yamaguchi K, Itokawa Y, Kikuno RF, Koga H, Ohara O. Exploration of human ORFeome: high-throughput preparation of ORF clones and efficient characterization of their protein products. *DNA Res*. 2008;15:137–149.
27. Gulick J, Subramania A, Neumann J, Robbins J. Isolation and characterization of the mouse cardiac myosin heavy chain genes. *J Biol Chem*. 1991;266:9180–9185.
28. Tardiff JC, Hewett TE, Factor SM, Vikstrom KL, Robbins J, Leinwand LA. Expression of the beta (slow)-isoform of MHC in the adult mouse heart causes dominant-negative functional effects. *Am J Physiol Heart Circ Physiol*. 2000;278:H421–H429.
29. Warren C, Greaser M. Method for cardiac myosin heavy chain separation by sodium dodecyl sulfate gel electrophoresis. *Anal Biochem*. 2003;320:149–181.
30. Pugach E, Richmond P, Azofeifa J, Dowell R, Leinwand L. Prolonged Cre expression driven by the α-myosin heavy chain promoter can be cardiotoxic. *J Mol Cell Cardiol*. 2015;86:54–61.
31. Robbins TW, James M, Owen AM, Sahakian BJ, Lawrence AD, McInnes L, Rabbitt PM. A study of performance on tests from the CANTAB battery sensitive to frontal lobe dysfunction in a large sample of normal volunteers: implications for theories of executive functioning and cognitive aging. Cambridge Neuropsychological Test Automated Battery. *J Int Neuropsychol Soc*. 1998;4:474–490.
32. Naiman RJ, Alldredge JR, Beauchamp DA, Bisson PA, Congleton J, Henny CJ, Huntly N, Lamberson R, Levings C, Merrill EN, Pearcy WG, Rieman BE, Ruggerone GT, Scarnecchia D, Smouse PE, Wood CC. Developing a broader scientific foundation for river restoration: Columbia River food webs. *Proc Natl Acad Sci USA*. 2012;109:21201–21207.
33. Crocini C, Ferrantini C, Scardigli M, Coppini R, Mazzoni L, Lazzeri E, Pioner JM, Scellini B, Guo A, Song LS, Yan P, Loew LM, Tardiff J, Tesi C, Vanzi F, Cerbai E, Pavone FS, Sacconi L, Poggesi C. Novel insights on the relationship between T-tubular defects and contractile dysfunction in a mouse model of hypertrophic cardiomyopathy. *J Mol Cell Cardiol*. 2016;91:42–51. DOI: 10.1016/j.yjmcc.2015.12.013.
34. Palermo J, Gulick J, Colbert M, Fewell J, Robbins J. Transgenic remodeling of the contractile apparatus in the mammalian heart. *Circ Res*. 1996;78:504–509.
35. Lucas D, Aryal P, Szweda L, Koch W, Leinwand L. Alterations in mitochondrial function in a mouse model of hypertrophic cardiomyopathy. *Am J Physiol Heart Circ Physiol*. 2003;284:H575–H583.
36. van der Velden J, Tocchetti C, Varricchi G, Bianco A, Sequeira V, Hilfiker-Kleiner D, Hamdani N, Leite-Moreira A, Mayr M, Falcão-Pires I, Thum T, Dwason D, Balligand J, Heymans S. Metabolic changes in hypertrophic cardiomyopathies: scientific update from the Working Group of Myocardial Function of the European Society of Cardiology. *Cardiovasc Res*. 2018;114:1273–1280.
37. Lim C, Apstein C, Colucci W, Liao R. Impaired cell shortening and relengthening with increased pacing frequency are intrinsic to the senescent mouse cardiomyocyte. *J Mol Cell Cardiol*. 2000;32:2075–2082.
38. Landrum M, Lee J, Benson M, Brown G, Chao C, Chitipiralla S, Gu B, Hart J, Hoffman D, Jang W, Karapetyan K, Katz K, Liu C, Maddipatla Z, Malheiro A, McDaniel K, Ovetsky M, Riley G, Zhou G, Holmes J, Kattman B, Maglott D. ClinVar: improving access to variant interpretations and supporting evidence. *Nucleic Acids Res*. 2018;46:D1062–D1067.
39. Lee LA, Karabina A, Broadwell LJ, Leinwand LA. The ancient sarcomeric myosins found in specialized muscles. *Skelet Muscle*. 2019;9:7.
40. Stauffer BL, Konhilas JP, Luczak ED, Leinwand LA. Soy diet worsens heart disease in mice. *J Clin Invest*. 2006;116:209–216.
41. Haines CD, Harvey PA, Luczak ED, Barthel KK, Konhilas JP, Watson PA, Stauffer BL, Leinwand LA. Estrogenic compounds are not always cardioprotective and can be lethal in males with genetic heart disease. *Endocrinology*. 2012;153:4470–4479.
42. Trépanier-Boulay V, St-Michel C, Tremblay A, Fiset C. Gender-based differences in cardiac repolarization in mouse ventricle. *Circ Res*. 2001;89:437–444.
43. Parks R, Ray G, Bienvenu L, Rose R, Howlett S. Sex differences in SR Ca(2+) release in murine ventricular myocytes are regulated by the cAMP/PKA pathway. *J Mol Cell Cardiol*. 2014;75:162–173.
44. Lange S, Xiang F, Yakovenko A, Vihola A, Hackman P, Rostkova E, Kristensen J, Brandmeier B, Franzen G, Hedberg B, Gunnarsson LG, Hughes SM, Marchand S, Sejersen T, Richard I, Edstrom L, Ehler E, Udd B, Gautel M. The kinase domain of titin controls muscle gene expression and protein turnover. *Science*. 2005;308:1599–1603.

SUPPLEMENTAL MATERIAL

Table S1. Observed distribution of live births by genotype of MYH7b +/+, MYH7b +/-, and MYH -/- mice after breeding of MYH7b +/- mice.

	Number	Ratio (%)
MYH7b+/+	**56**	**22.4**
MYH7b+/-	**139**	**55.6**
MYH7b-/-	**55**	**22.0**
Total	**250**	**100.0**

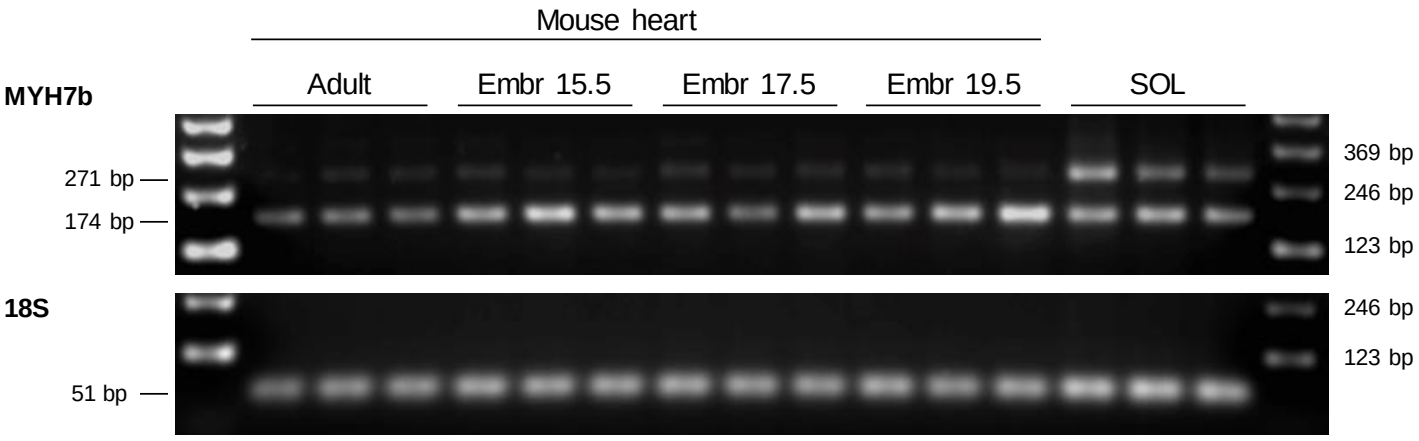

Figure S1. RT-PCR assessment of MYH7b exon 7 skipping/inclusion and 18S as a normalizing control. Samples as indicated. Soleus was included as a positive control for inclusion of exon 7 as MYH7b protein is expressed in muscle spindles of the soleus muscle.

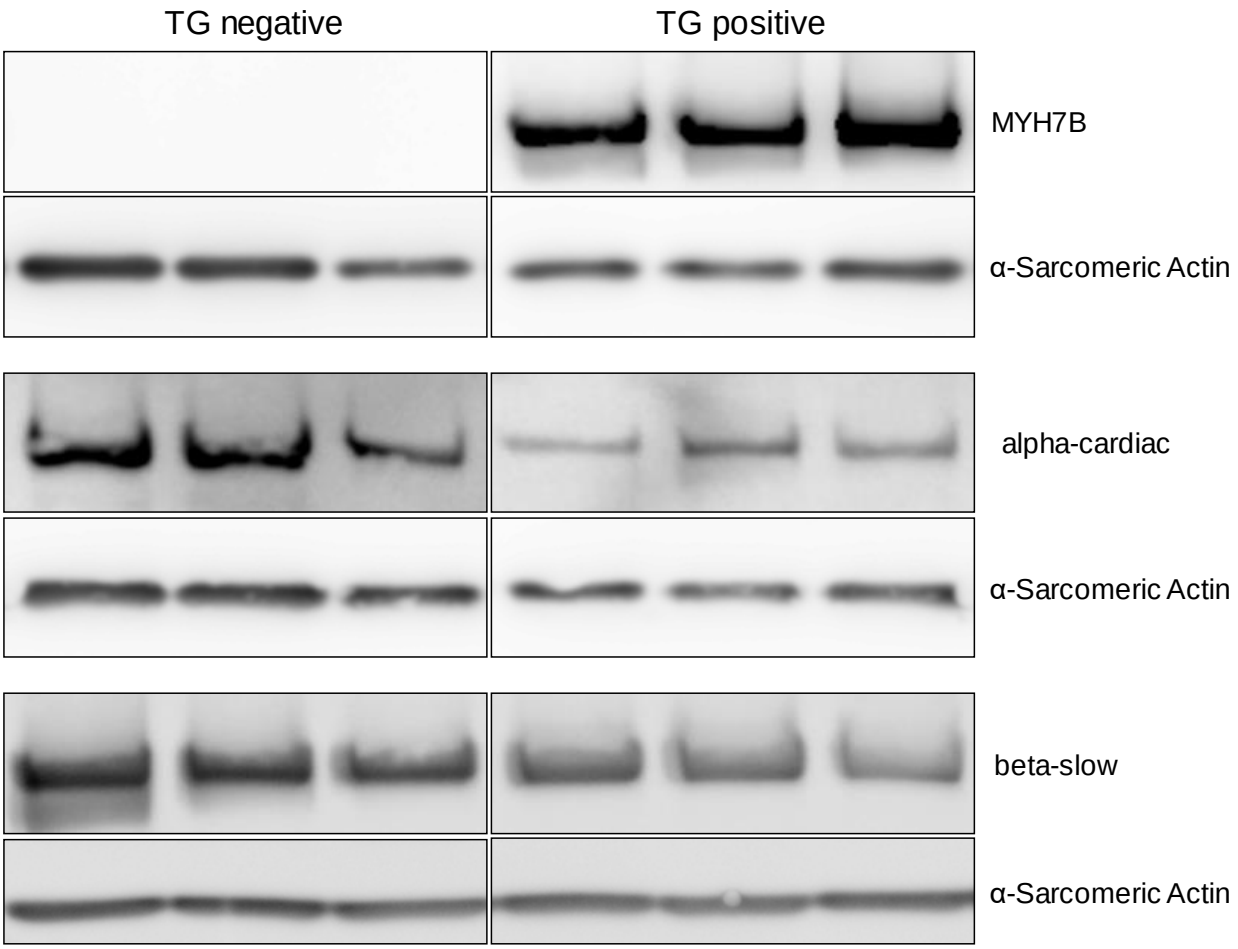

Figure S2. Myc-tagged MYH7b expression in LV's of α-MYH7b transgenic mice. LV protein extracts from 7 month-old male mice were blotted for the presence of MYH7b (detected by Myc-tag antibody). Other sarcomeric components were detected by antibodies as indicated. Sarcomeric actin was used as a loading control.

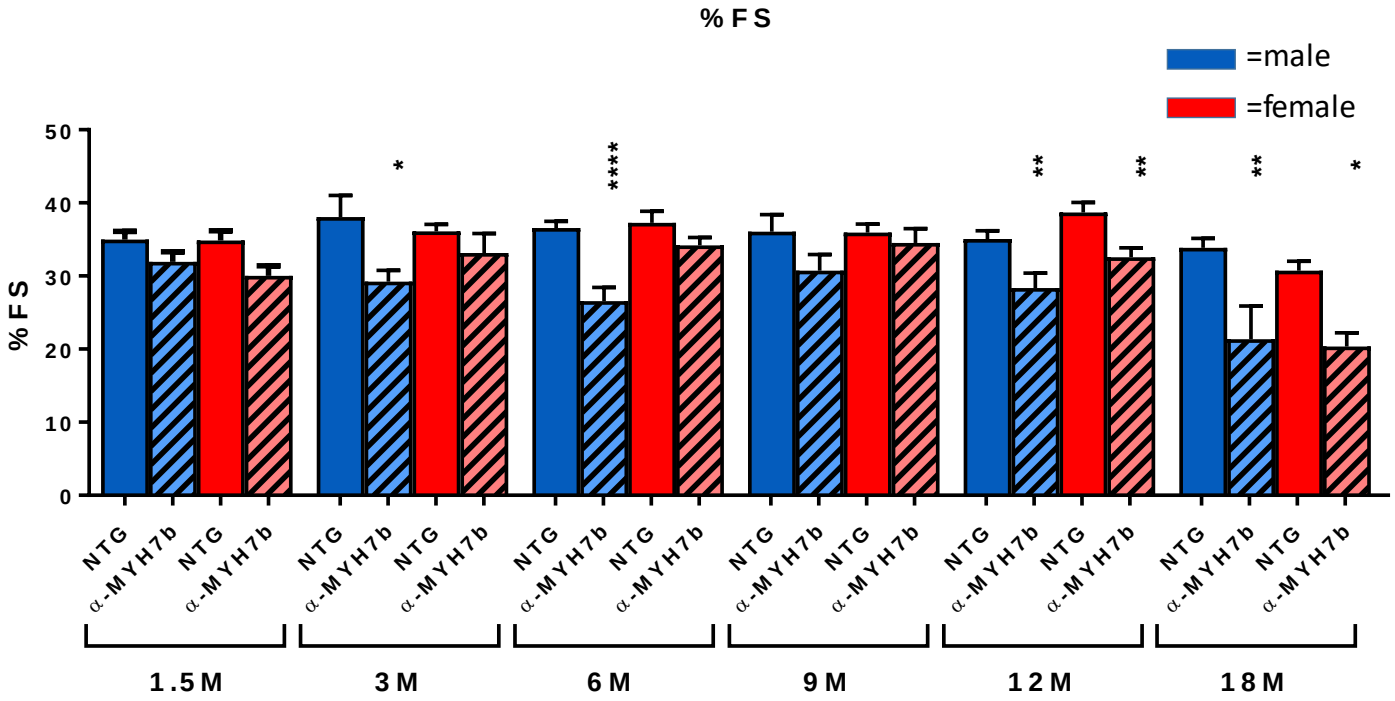

Figure S3. MYH7b expression results in early LV dysfunction in male and female α-MyH7b mice. Echocardiography profiles of 1.5, 3, 6, 9, 12, and 18 month-old male and female mice showing significant functional changes (%FS) in male mice beginning at 3 months-of-age, but female mice are protected from the development of cardiac dysfunction until 12 months-of-age. Student's t-test was performed between NTG and α-MYH7b transgenic mice at each age as indicated *P ≤ 0.05, **P ≤ 0.01, **** P ≤ 0.0001. Animal numbers reported in Tables 1 and 2. Animal numbers are as follows: **Males** 1.5M: NTG n=14, TG n=15; 3M: NTG n=5, TG n=13; 6M: NTG n=20, TG n=16; 9M: NTG n=10; TG n=13; 12M: NTG n=15, TG n=15; 18M: NTG n=12, TG n=6. **Females** 1.5M: NTG n=9, TG n=11; 3M: NTG n=9, TG n=12; 6M: NTG n=8, TG n=17; 9M: NTG n=10; TG n=12; 12M: NTG n=12, TG n=7; 18M: NTG n=10, TG n=17.

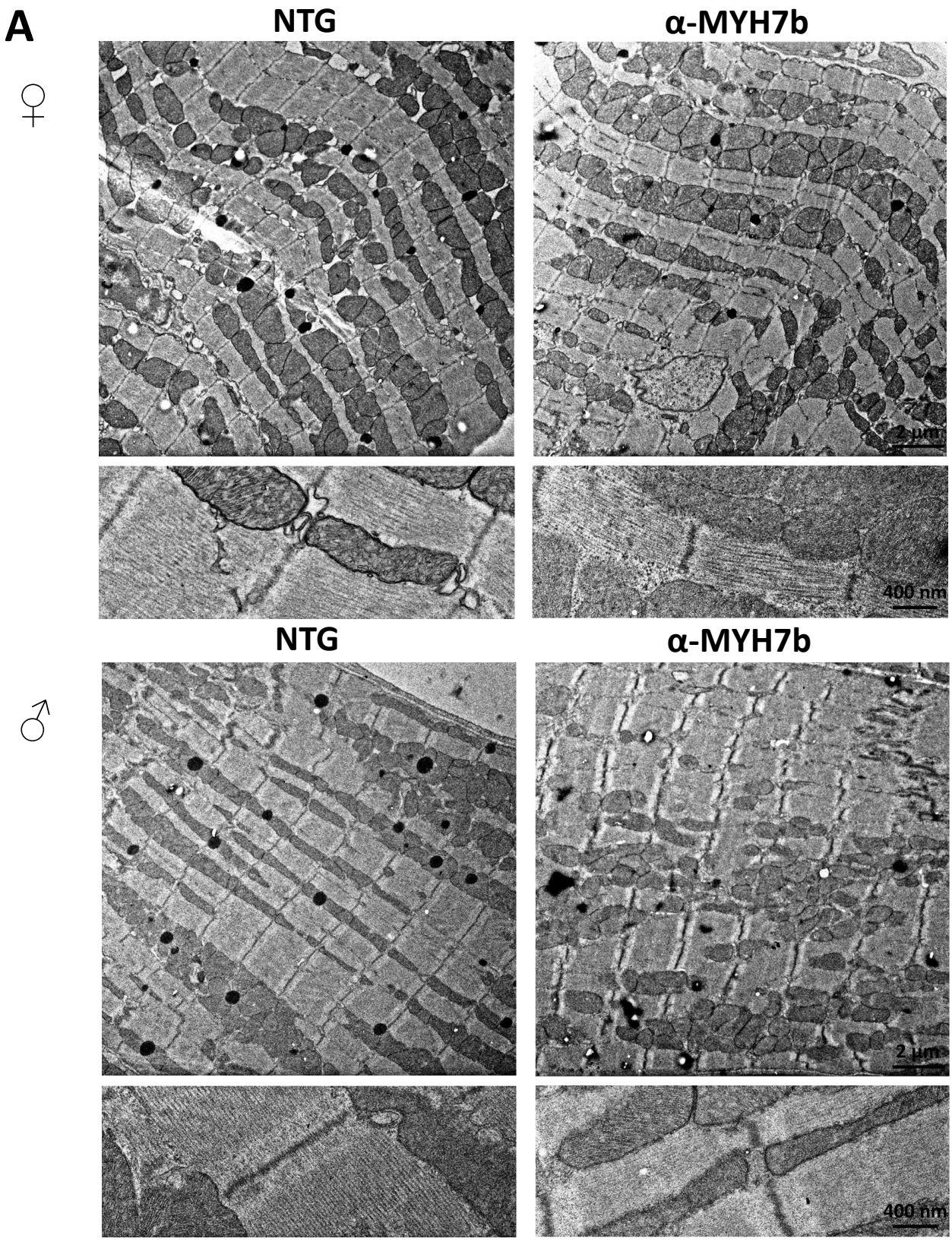
A
NTG
α-MYH7b
♀
2 µm
400 nm
NTG
α-MYH7b
♂
2 µm
400 nm

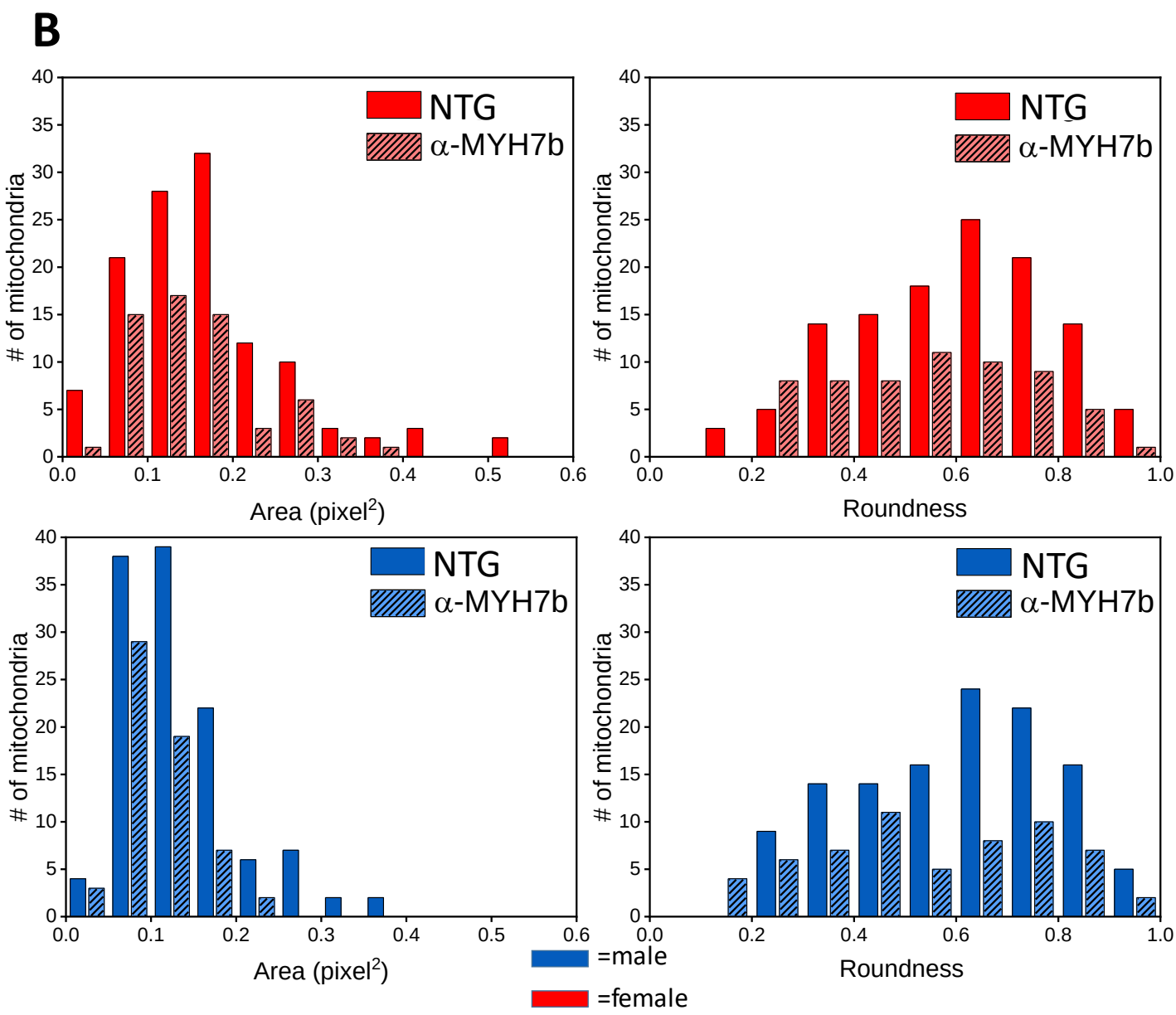

Figure S4. Analysis of area and roundness of mitochondria from 1.5 month-old mice. A. Representative electron microscopic (EM) images from 1.5 month-old both male and female NTG and α-MYH7b transgenic mice. Bar in upper panels = 2µm, Bar in lower panels = 400nm. **B.** Frequency distributions (# of mitochondria) for area and roundness with 12 and 10 bins, respectively, of equal sizes. Data obtained from electron microscopy images of males (lower panels) and females (upper panels). Data from 120 mitochondria for NTG males and females and 60 mitochondria for α-MYH7b males and females. Animal numbers: n=2 for NTG and n=1 for α-MYH7b.

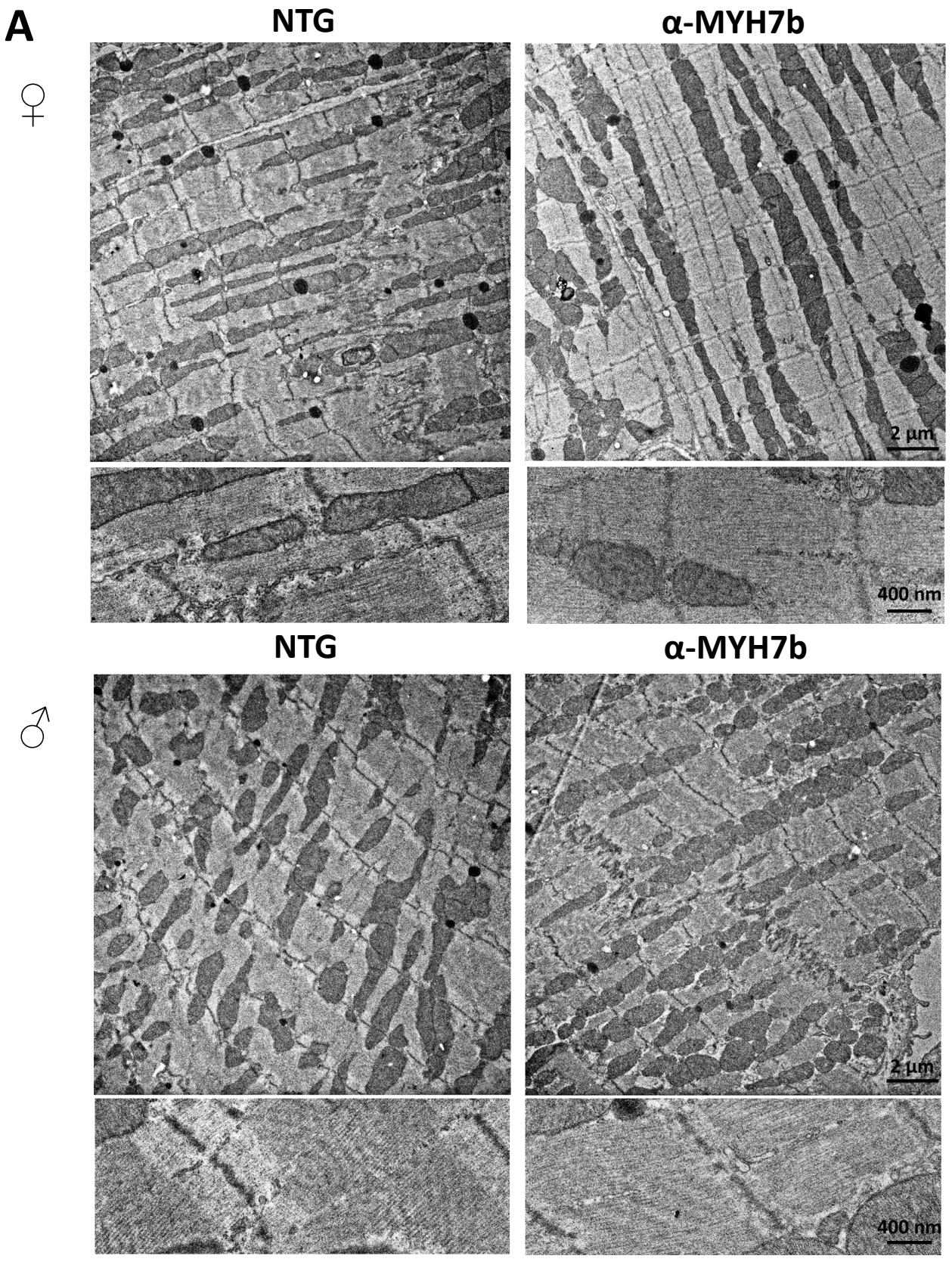
A
NTG
α-MYH7b
♀
2 µm
400 nm
NTG
α-MYH7b
♂
2 µm
400 nm

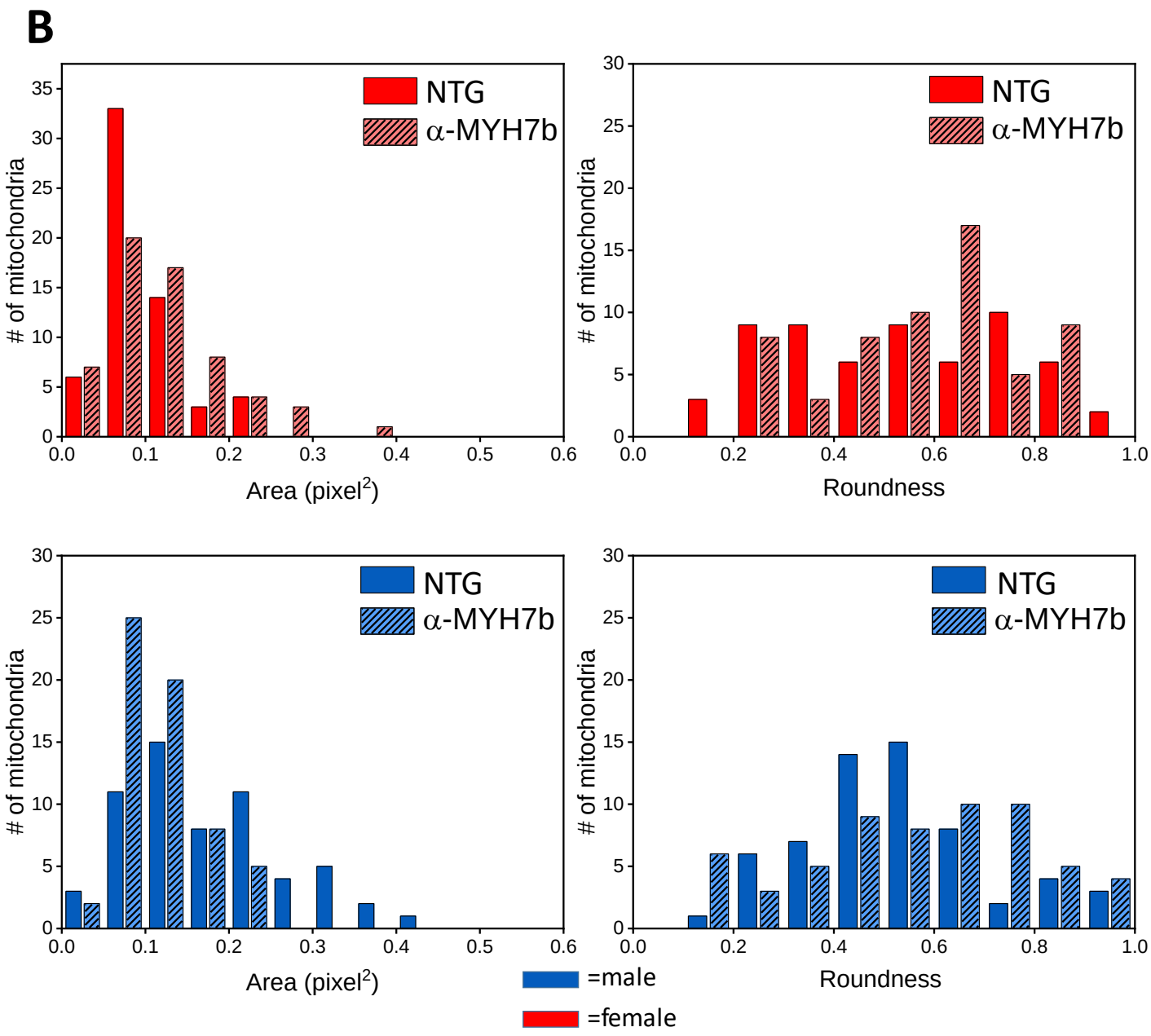

Figure S5. EM analysis of area and roundness of mitochondria from 18 month-old mice. A. EM images from 18 month-old both male and female NTG and α-MYH7b mice. Bar in upper panels = 2µm, Bar in lower panels = 400nm. **B.** Frequency distributions (# of mitochondria) for area and roundness with 12 and 10 bins, respectively, of equal sizes. Data obtained from electron microscopy images of males (lower panels) and females (upper panels). Data from 60 mitochondria for NTG and α-MYH7b transgenic male and female mice. Animal numbers: n=1 per group.

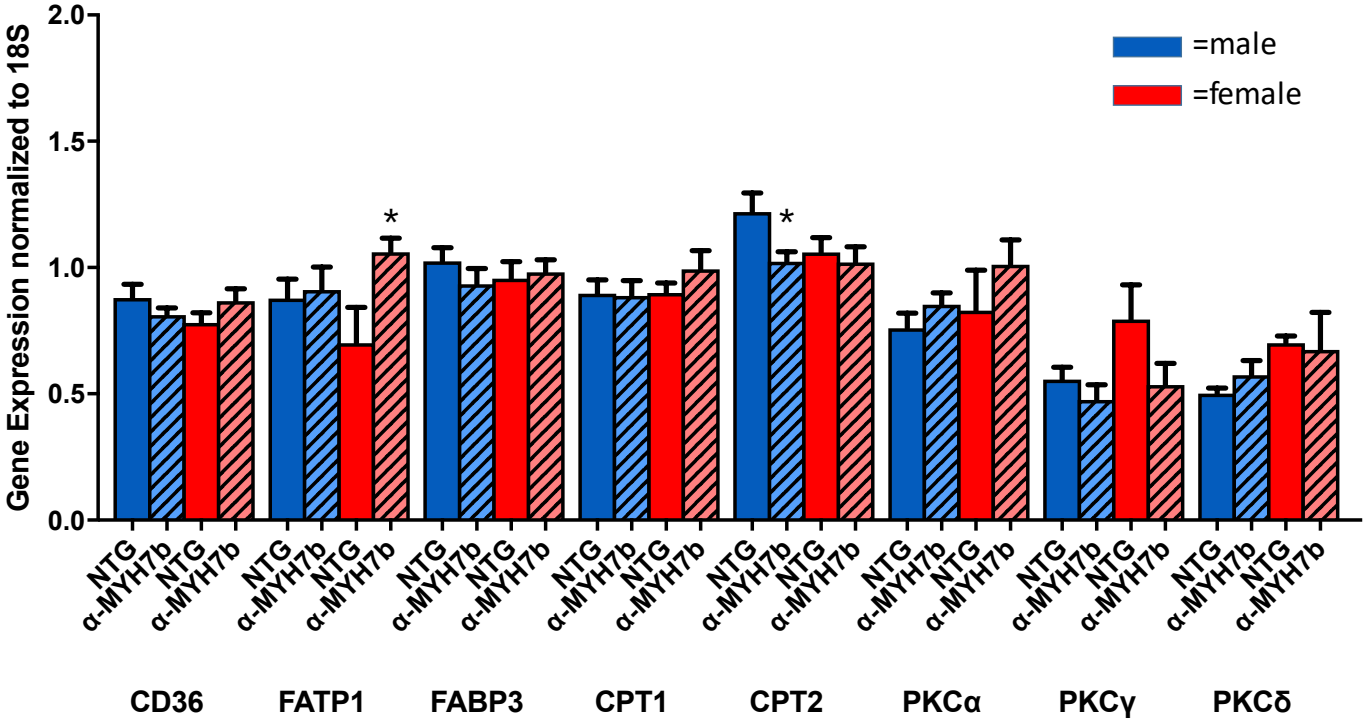

Figure S6. MYH7b expression does not result in substantial gene expression changes for fatty acid handling genes or pathological PKC isoforms. Gene expression analysis showing very few significant changes in genes at 1.5 months-of-age in either male or female transgenic (α-MYH7b) mice compared to their NTG littermates. Student's t-test was performed between NTG and α-MYH7b transgenic mice at each age indicated *P ≤ 0.05. Animal numbers: Male NTG n=9, Male α-MYH7b n=13, Female NTG n=3, Female α-MYH7b n=17.

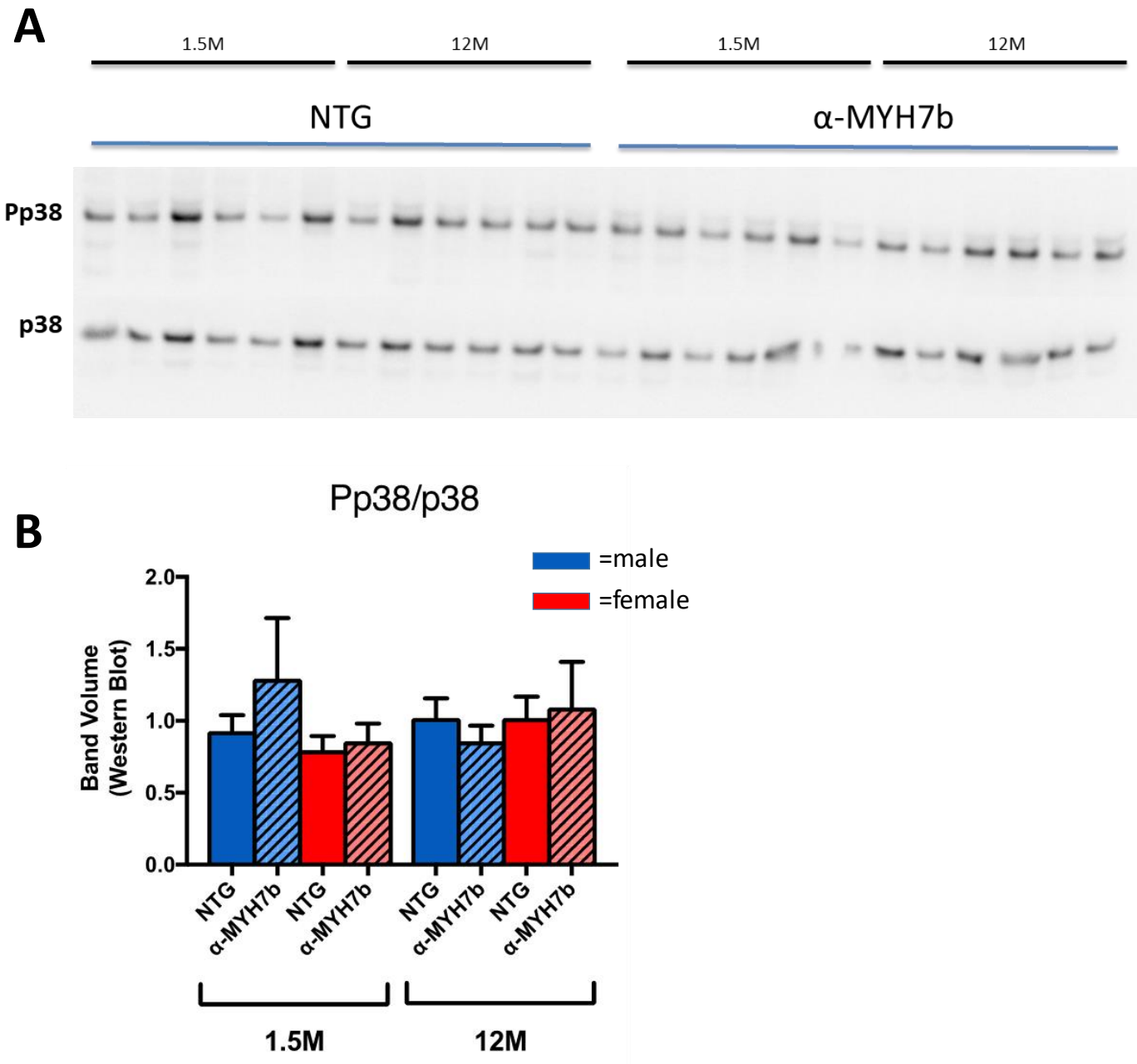

Figure S7. MYH7b cardiomyopathy is not associated with activation of the p38 pathway. A. LV protein extracts from 1.5 and 12 month-old male and female mice were blotted for the total (p38) and activated (Pp38) proteins. **B.** Quantitation of Western blots showed no significant activation of p38 pathway in either sex at 1.5 or 12 months-of-age. Animal numbers: n=3 NTG males, n=3 TG males, n=3 NTG females, n=3 TG females for each age group.

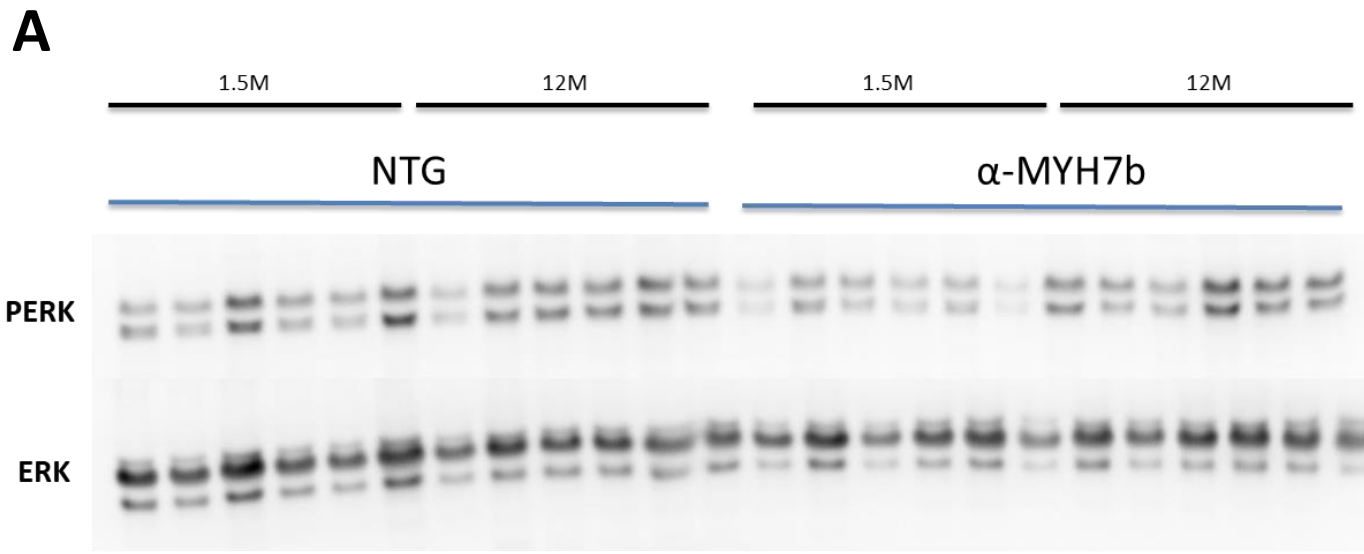

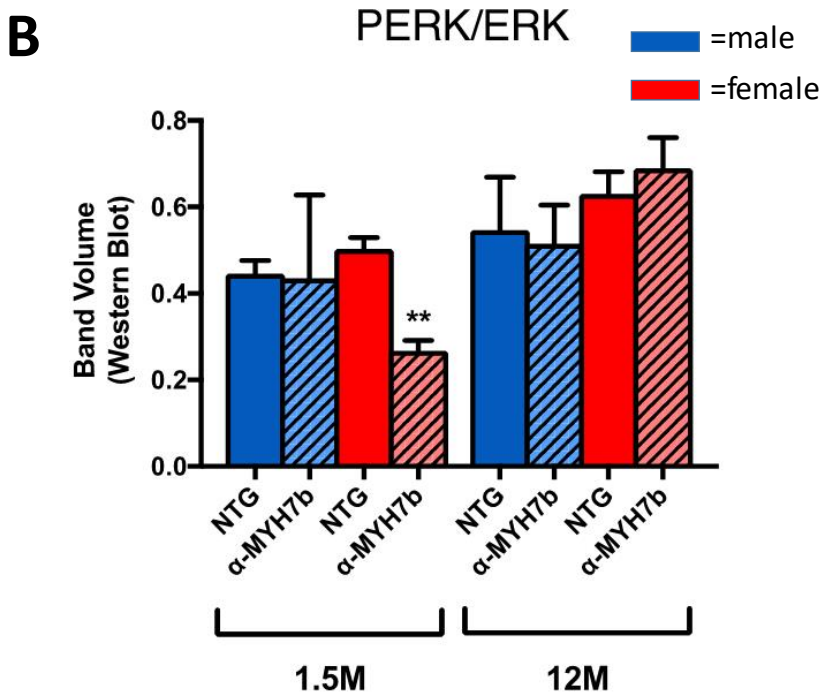

Figure S8. MYH7b expression is not associated with activation of the ERK pathway. A. LV protein extracts from 1.5 and 12 month-old male and female mice were blotted for the total (ERK) and activated (pERK) proteins. **B.** Quantitation of Western blots showed no significant activation of ERK pathway in α-MYH7b mice of either sex at 1.5 or 12 months-of-age and shows a significant reduction of pERK at 1.5 months-of-age in female α-MYH7b mice (using Student's t-test, **P ≤ 0.01). Animal numbers: n=3 NTG males, n=3 TG males, n=3 NTG females, n=3 TG females for each age group.